Wall Jet Scour in Rock

George W. Annandale[1], D.Ing., PE, F.ASCE

[1]Principal, Golder Associates, 44 Union Blvd, Suite 300, Lakewood, Colorado 80228; PH 303-980-0540; e-mail: george_annandale@golder.com

ABSTRACT

Rock scour by wall jets downstream of dams can compromise dam safety. The potential for such scour and its extent can be quantified by making use of the Erodibility Index Method (Annandale 1995; 2006). This method is based on a relationship between the stream power of flowing water and a geo-mechanical index representing the erosion resistance of the any earth material, ranging from non-cohesive and cohesive soils, to rock formations. In order to apply this method it is necessary to quantify the spatial distribution of the erosive capacity of wall jets, which can then be compared to the erosion resistance of the earth material under consideration. This paper presents a method that can be used to quantify the erosive capacity of wall jets and illustrates that the Erodibility Index Method can be used to quantify the maximum scour depth caused by wall jets.

INTRODUCTION

A scour threshold for all earth materials can be defined by relating the relative magnitude of the erosive capacity of flowing water to the relative ability of earth materials to resist erosion. (The terms erosion and scour are used interchangeably in this paper). Annandale (1995) published such a relationship (the Erodibility Index Method), which can be used to quantify for any earth material (from very fine sand, coarse sand and cobbles, through cohesive soils and vegetated earth material to intact rock formations) the potential and extent of scour for varying flow conditions (Annandale 2006).

This paper illustrates that the Erodibility Index Method can be used to quantify round wall jet scour potential and extent for non-cohesive sandy material. By extension it is concluded that the same approach can be used to quantify scour of rock subjected to wall jets. Analysis of rock scour by means of the Erodibility Index Method follows the exact same approach as applied to non-cohesive sandy material and has been shown by case studies to be successful in predicting scour potential and extent in any earth material (Annandale 2006).

PREVIOUS RESEARCH APPROACH

Historically, wall jet scour research relates dimensionless maximum scour depth to the dimensionless densimetric Froude number (e.g. Ade and Rajaratnam 1998; Aderibigbe & Rajaratnam 1999; and others). The densimetric Froude number is expressed as,

$$F_o = \frac{U_o}{\sqrt{g\frac{(\rho_s - \rho)}{\rho}d_*}} \quad (1)$$

Where U_o = jet velocity at nozzle (m/s); g = acceleration due to gravity (m/s^2); ρ_s = mass density of sediment (kg/m^3); ρ = mass density of water (kg/m^3); d_* = characteristic sediment particle diameter (m).

The research results from this approach have limited practical application because it may only be used to assess scour in non-cohesive earth material. It is not possible to relate the findings of that research to scour potential of other earth materials like cohesive soils or rock masses.

PROPOSED APPROACH

This paper follows a cause-and-effect approach instead of the conventional densimetric Froude number approach. The relative magnitude of the erosive capacity of the wall jet is determined by quantifying its stream power, and the relative magnitude of the erosion resistance of the earth material is quantified using the Erodibility Index Method (Annandale 1995; 2006). Annandale's erosion threshold is then used to assess for the earth material scour potential and extent.

The paper is presented in two parts. The first part describes the methodologies used to quantify the erosive capacity of wall jets and the erosion resistance of earth materials and, through a cause-and-effect approach, quantify erosion depth. The second part of the paper uses published research results by Ade and Rajaratnam (1998) to validate the method.

EROSION RESISTANCE AND EROSIVE CAPACITY

Erosion is deemed to occur when the erosive capacity of the flowing water exceeds the erosion resistance of an earth material; and is deemed to cease when the erosion resistance of the earth material exceeds the erosive capacity of the flowing water. By following this approach the maximum depth of scour is determined with known spatial distributions of the erosive capacity of flowing water and the erosion resistance of the earth material.

Quantification of erosive capacity of Wall Jets

Albertson et al. (1950) provides a detailed analysis of the diffusion of round submerged jets, indicating that the flow downstream of the issuance point consists of two flow zones, i.e. a zone of flow establishment and a zone of established flow (Figure 1). The zone of flow establishment is dominated by the core of the jet, which gradually diminishes in size as a function of distance from the issuance point. Within the zone of flow establishment the maximum flow velocity, i.e. the flow velocity in the core, remains constant and equals the jet issuance velocity.

Once the flow proceeds beyond the zone of flow establishment its movement is maintained by the momentum introduced by the jet. In this zone the maximum velocity gradually reduces and the rate of jet spread increases. Albertson et al. (1950) quantify the spatial distribution of flow velocity at right angles to the jet by assuming

that the lateral reduction in flow velocity follows a Gaussian distribution. They derived continuity, momentum and energy equations for jet flow into an infinite medium.

Albertson et al. (1950) derived the relationship between dimensionless shear stress and dimensionless space for the established flow zone (Figure 2). The figure relates $\frac{100 \cdot \tau}{\rho \cdot v_{max}^2}$, the dimensionless shear stress, and $\frac{r}{x}$, the dimensionless distance; where τ = shear stress (Pa); ρ = fluid density (kg/m^3); v_{max} = maximum flow velocity (m/s); r = variable radius at right angles to the jet axis (m); x = distance along the jet axis (m).

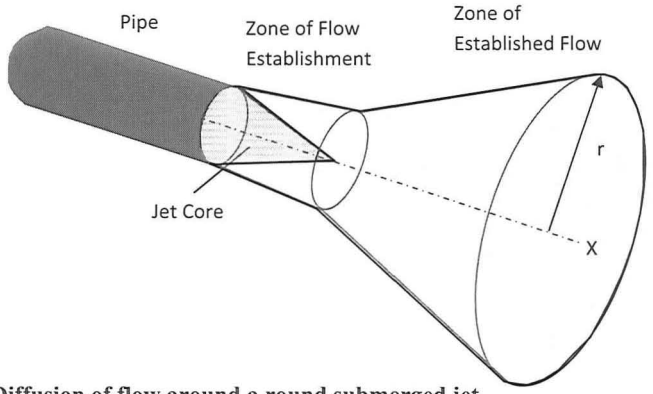

Figure 1 Diffusion of flow around a round submerged jet

For a round jet the equation for calculating the maximum flow velocity in the established flow zone is (Albertson et al. 1950):

$$v_{max} = 6.2 \cdot \frac{D_o}{x} \cdot v_o \tag{2}$$

Where D_o = jet diameter at issuance (m); v_o = issuance jet velocity (m/s).

The shear stress produced by the round submerged jet is calculated as,

$$\tau\left(\frac{r}{x}\right) = f \cdot \rho \cdot \frac{v_{max}^2}{100} \tag{3}$$

Where f = functional relationship between $\frac{100 \cdot \tau}{\rho \cdot v_{max}^2}$ and $\frac{r}{x}$ for a round jet presented in Figure 2.

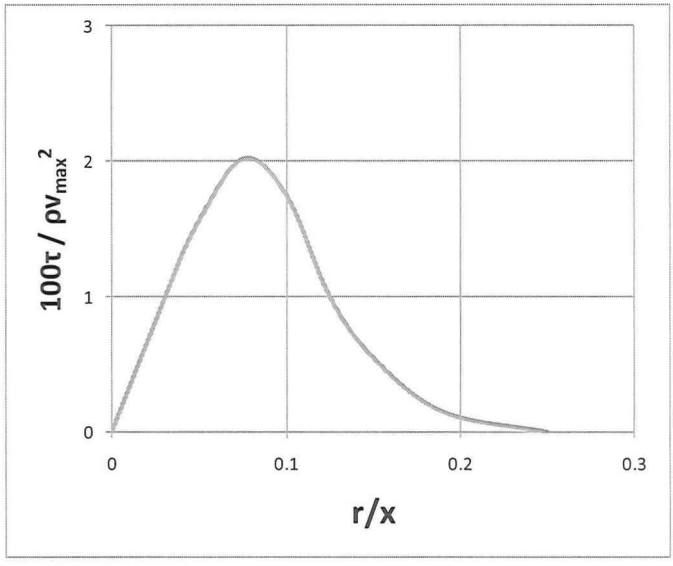

Figure 2 Relationship between transverse dimensionless shear stress and dimensionless space in the established flow zone for round jets discharging into a fluid with infinite depth (Albertson et al. 1950)

Equations (2) to (3) represent flow variables for a jet submerged in water with infinite depth, i.e. its flow are not affected by solid boundaries. When this condition is changed by placing a boundary parallel to the x-axis it affects the flow conditions. The jet's erosive capacity along such a boundary can be determined by quantifying the turbulence production in the near-bed region along that boundary.

Schlichting and Gersten (2000) provide the distribution of turbulence production in the near-bed region along a boundary (Figure 3). It relates dimensionless energy supply, turbulence production and direct (viscous) energy dissipation to dimensionless flow depth.

Dimensionless turbulence production, quantified on the ordinate of Figure 3, is expressed

as $\tau^+ \frac{du^+}{dy^+}$; where $\tau^+ = \frac{\tau_t}{\rho u_*^2}$; τ_t = turbulent shear stress at the boundary (Pa); $u_* = \sqrt{\frac{\tau}{\rho}}$ = shear velocity (m/s); τ = average wall shear stress (Pa). $u^+ = \frac{\overline{u}}{u_*}$; where $\overline{u}$ = average flow velocity (m/s).

The abscissa on Figure 3 is $y^+ = \frac{y}{\delta}$; where y = variable flow depth (m); δ = wall layer thickness, defined as $\delta = \frac{\nu}{u_*}$; where ν = kinematic viscosity of the water (m^2/s).

By integrating the dimensionless relationship between $\tau^+ \frac{du^+}{dy^+}$ and y^+ Annandale (2006) showed that the applied stream power $\tau_t \cdot \overline{u}$ (watt/m^2) in the near-bed region along a boundary can be expressed as

$$\tau_t \cdot \overline{u} = 7.853\rho\left(\frac{\tau}{\rho}\right)^{3/2} \tag{4}$$

Inserting the shear stress determined with Equation (3) into Equation (4) it is possible to quantify the applied stream power $P\left(\frac{r}{x}\right)$ (watt/m^2) for a round jet along a boundary, i.e.

$$P\left(\frac{r}{x}\right) = 7.853 \cdot \rho \cdot \left(\frac{\tau\left(\frac{r}{x}\right)}{\rho}\right)^{3/2} \tag{5}$$

For round jets the length of the flow establishment zone is (Albertson et al. 1950),

$$x_o = \frac{D_o}{2 \cdot C_1} \tag{6}$$

where $C_1 = 0.109$.

Therefore, the distance along the x-axis x' (m) where shear stress and the applied stream power is calculated is quantified as,

$$x' = x + x_o \tag{7}$$

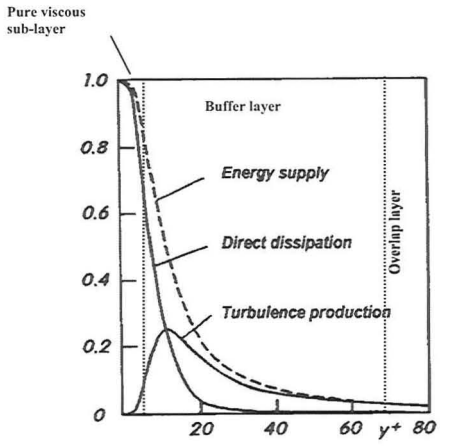

Figure 3 Universal energy balance of the mean motion in the near-bed region (Annandale 2006)

Quantification of erosion resistance

The Erodibility Index Method (Annandale 1995; 2006) provides an approach to quantify the erosion resistance of any earth material, ranging from non-cohesive to cohesive and vegetated soils, to intact rock formations (Figure 4). The erosion threshold relates stream power and the Erodibility Index K, which is defined as,

$$K = M_s \cdot K_b \cdot K_d \cdot J_s \tag{8}$$

Where M_s = mass strength number (-); K_b = block size number (-); K_d = inter-block / inter-particle shear strength number (-); J_s = shape and orientation number (-).

Methods to quantify the numbers making up the Erodibility Index are presented in Annandale (1995; 2006) and are not repeated here in full. The mass strength number, which can be obtained from tables published in Annandale (2006), assumes a value of about 0.02 for very loose non-cohesive soil.

The block size number for non-cohesive earth material is quantified as,

$$K_b = 1000 \cdot d^3 \tag{9}$$

The inter-particle shear strength number is calculated as,

$$K_d = \tan\phi$$

Where ϕ = internal angle of friction of the non-cohesive soil.

By convention, in the case of soils, the shape and orientation number J_s = 1.0.

The threshold stream power for a particular earth material is determined using Figure 4 or by using either of the following equations,

$$P_t = K^{3/4} \quad \text{for } K \geq 0.1 \tag{10}$$

or

$$P_t = 0.48 \cdot K^{0.44} \quad \text{for } K < 0.1 \tag{11}$$

Where P_t = threshold stream power (kW/m^2).

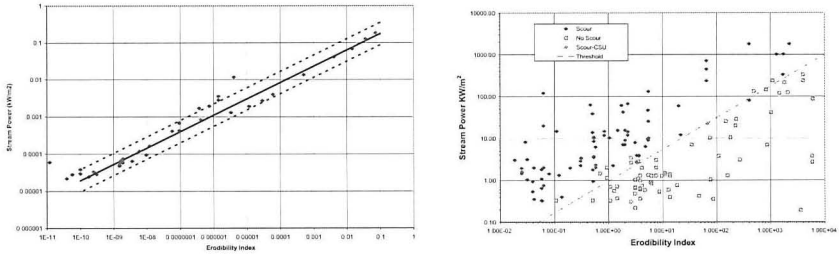

Figure 4 Erosion threshold for earth materials defined by the Erodibility Index and stream power (Annandale 1995; 2006); Figure on left are for K < 0.1 and that on the right is for K ≥ 0.1

Scour Depth Quantification

Calculation of scour depth proceeds by comparing the threshold stream power P_c and the applied stream power $P\left(\frac{r}{x}\right)$ for round jets. When the applied stream power exceeds the threshold stream power, scour is deemed to occur; and when the applied stream power is less than the threshold stream power, scour is deemed to cease. This approach is used to quantify both maximum scour depth and its location (Figure 5). This figure illustrates the spatial distribution of stream power as a function of the longitudinal distance x along the jet axis and the radial distance r around the jet axis.

The graph on the left has a smaller base than that on the right. The reason for this is that the lowest value on the vertical axis, representing the threshold stream power, is 30 watt/m^2 on the left hand graph and 10 watt/m^2 on the right hand graph. *For purposes of illustration* these values respectively represent the threshold stream power for two alternate materials. The base of the graph provides an indication of the scour extent as a function of x and r because the applied stream power below the two respective horizontal planes (30 and 10 watt/m^2 respectively) is lower than the threshold stream power represented by those planes.

The maximum scour depth on the left hand graph is approximately 0.05m and it occurs at a distance of about 0.6m from the point of issuance. For the right hand

graph the maximum scour depth is about 0.075m and it occurs about 0.75m from the point of issuance. This procedure has been followed to calculate scour depths for experimental data from Ade and Rajaratnam (1998) for round jets.

RESULTS

Figure 6 compares calculated and observed scour depth using the Erodibility Index Method erosion resistance criterion. It is noted that the 25mm jet in high tailwater provides a good correlation, while the 5mm jet in high tailwater provides less satisfactory results. It is also noted that both the 19mm and 25mm jets in low tailwater results in higher calculated than observed scour depths.

These results are interpreted to mean that the erosive capacity of the jets is more accurately represented in high tailwater, which more closely represents the conditions analyzed by Albertson et al. (1950), i.e. infinite water depth. The discrepancy observed for the 5mm jet, although in high tailwater, is attributed to a scaling problem. The 5mm jet used by Ade and Rajaratnam (1998) is very small compared to the non-cohesive soil sizes used in those experiments.

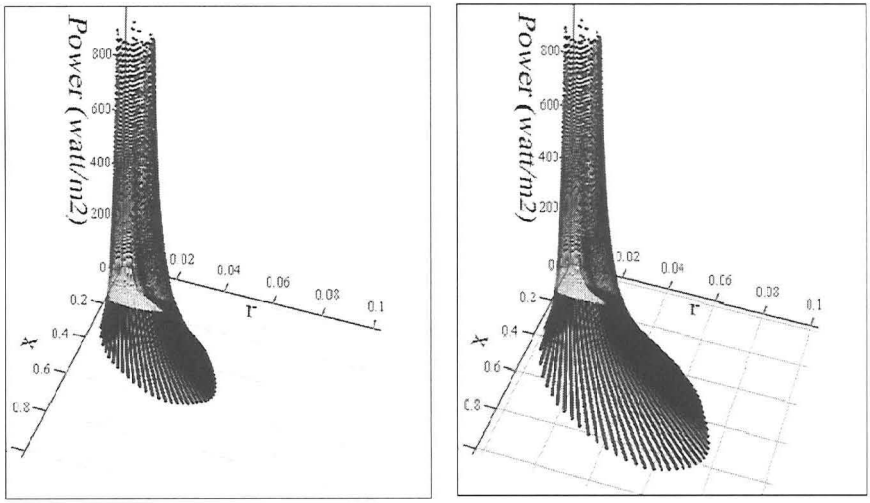

Figure 5 Determination of scour depth and distance for two alternative earth materials. The figure on the left represents an earth material with an erosion threshold equaling 30 watt/m^2 and the figure on the right for a material with erosion threshold equaling 10 watt/m^2.

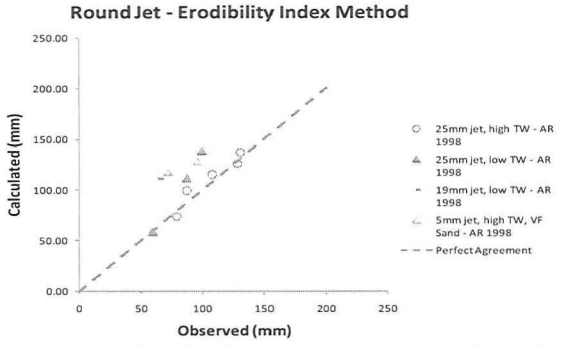

Figure 6 Comparison between calculated and observed scour depths in uniform, non-cohesive sediment for round jets.

CONCLUSION

The correlation between observed and calculated scour depths using Albertson et al. (1950) to quantify stream power and the Erodibility Index (Annandale 1995; 2006) to quantify scour resistance is satisfactory for non-cohesive soils. No scour data for wall jet scour in rock is known to the author.

Based on previous experience using the Erodibility Index Method and on the fact that the erosion threshold defined by this method is continuous it is deemed reasonable to assume that rock scour due to wall jets can be assessed using the same approach. The Erodibility Index Method is a cause-and-effect approach. By quantifying the spatial distribution of the erosive capacity of a wall jet and the spatial distribution of the erosion threshold of any earth material (including rock), using the Erodibility Index Method, makes is possible to estimate scour potential and extent. The scour threshold presented in Figure 4 for all earth materials can be used to estimate scour potential and extent of scour caused by wall jets, based on the concept presented in Figure 5.

REFERENCES

Ade, F. and Rajaratnam, N. 1998. Generalized study of erosion by circular horizontal turbulent jets, J. Hydr. Eng. 124(10), 1034-1042.

Albertson, M.L., Dia, Y.B., Jensen, R.A. and Rouse, H. 1950. Diffusion of submerged jets, Transactions of the ASCE, Vol. 150, 639-664.

Annandale, G.W. 2006. Scour Technology, McGraw-Hill, New York.

Annandale, G. W. (1995), Erodibility, Journal of Hydraulic Research, vol. 33, No. 4, pp. 471 – 494.

Soft-Rock Scouring Processes Downstream of Weirs

Cheng, M.-H.[1,2], Liao, J.-J.[1], Pan, Y.-W.[1],
Li, G.-W.[1], Huang, M.-W.[1], Lo, W.-H.[1], Hsu, S.-T.[2]

[1]Department of Civil Engineering, National Chiao-Tung University, 1001 Ta-Hsueh Rd., Hsinchu 30050, Taiwan; email: jjliao@mail.nctu.edu.tw
[2]Water Resources Agency, Ministry of Economic Affairs, 1340, Jhong-Jheng Rd., Wufong Township, Taichung County 413, Taiwan; email: chengms@wrap.gov.tw

ABSTRACT

Diversion weirs are typically constructed to elevate river water levels and thereby increase water supplies. Most riverbeds in the western foothills of Taiwan are composed of soft sedimentary rocks covered with an armor layer of varying thickness. Due to the low rock strength and head fall caused by weirs, rapid scouring downstream of the weir often occurs once the armor layer is worn away. To estimate scour depth and mitigate its damage to weir foundations, scouring processes must be identified correctly. Because of different mechanical behaviors and the water-jet conditions, scouring processes downstream of a weir on soft rock may not be that same as those assumed by existing models. Analytical results from a series of studies of scouring downstream of weirs on soft rock indicate that the shape of a scour hole on soft rock differs markedly from that of a scour hole on hard rock. This study identified three basic scouring processes downstream of weirs, namely, (1) plucking, (2) uniform incision, and (3) trenching incision. The suitability of existing approaches for calculating the depth of a scour hole on soft rock were also assessed.
Keywords: scouring processes; soft rock; weir; scour hole

INTRODUCTION

Diversion weirs were typically constructed across rivers in Taiwan to elevate the river level to increase water supply. These weirs alter the nearby river slope and result in loss of the armor layer; the rock mass downstream of the weirs is then exposed. Also, the extra flow energy due to the head fall enhances rock cracking or breakage, and a scour hole may then develop gradually. Eventually, scouring may reach an extent that weir stability is endangered.

The common erosion mechanisms in a rock bed can be classified as plucking, abrasion, and cavitation. The major mechanism depends on substrate lithology, joint spacing, fractures, and bedding planes. Plucking is the dominant scouring mechanism when rocks are well jointed on a sub-meter scale. Abrasion is the result of wearing by a suspended load or saltating bedload. Cavitation occurs when a water environment has a high-speed vortex (Whipple 2000).

Many empirical or semi-empirical formulae for estimating the depth of a scour hole in a granular riverbed were developed using experimental data in the laboratory or field (e.g., Schoklitsch, 1932). The parameters used in those formulae may include grain size, flow rate, flow velocity, flow impact angle, and fall height. Among these parameters, grain size is the only material parameter that characterizes the geo-material of a riverbed.

To estimate the depth of scour holes in rocks, many studies directly adopted approaches used for granular materials. The bed material is simply taken as a cohesionless granular material when estimating the depth of a scour hole in a rock bed. Such approaches assume the rock mass is broken and all rock blocks are fully separated. Similar to cases for granular materials, the shape of a scour hole downstream is a slope with a constant angle related to the friction angle of the material. The depth of a scour hole can be calculated using the critical incipient shear stress law or the principal of conservation (Fahlbusch, 1994; Bormann, 1991; Liu, 2005). However, such approaches cannot closely predict the scouring potential of rock materials or rock masses.

Evaluating the scouring process for a rock mass is more complex than that for granular materials. Annandale developed a geo-mechanical index method; an erodibility index was utilized to quantify relative rock resistance to scouring (Annandale 1995). The erodibility index accounts for such factors as unconfined compressive strength, block size, shear strength of discontinuity, and the orientation of the discontinuities relative to flow. With the correlation between threshold stream power and the erodibility index, one can evaluate scouring susceptibility for a specific site as long as stream power at that site can be calculated from unit flow rate and fall height. Annandale (Annandale 2006) also utilized this method to estimate ultimate scour depth. With height of the tail water as constant, erosive power decreases as water depth increases because of energy dissipation. The erodibility index may vary (often increases) as water depth increases. Consequently, at a certain

depth, erosive power cannot overcome rock resistance to erosion; thus, scour depth can be estimated accordingly.

The fluctuating dynamic jet pressure and its propagation into rock joints have been discussed since the 1960s. Bollaert and Schleiss (2003) summarized the physical-mechanical processes of scouring as the following modules: (1) aerated jet impact; (2) jet diffusion in a plunge pool; (3) fluctuating dynamic pressures at the water-rock interface; (4) propagation of these pressures into underlying rock joints and hydraulic fracturing of the rock; (5) dynamic uplift of single rock blocks; and, (6) downstream mounding of material. They adopted two-dimensional jet diffusion theory to estimate the fluctuating dynamic pressure on rock surfaces, and the ratio of pressure amplification in joints. Scour depth can be estimated based on the force equilibrium of rock blocks. They used this approach to estimate scour depth and apron concrete thickness in plunge pools, where bedrocks are hard and jointed (Bollaert 2003).

Generally, most approaches for estimating scour depth were developed for plunge pools downstream of dams. In this case, the magnitude of jet energy depends on dam height, and energy dissipation follows two-dimensional diffusion theory. However, a diversion weir is typically submerged during flooding because the fall height of weirs is limited. Compared with high dams, the jet impinges a relatively small angle incline relative to the horizontal plane. The energy dissipation mechanism in front of a diversion weir may differ from that in the case of a jet falling from a spillway. Lin (2001) conducted a series of flume tests and characterized the formation of a scour hole caused by a low hydraulic jump. The depth and shape of the developed scour hole depend on flow conditions and tail water depth.

Most riverbeds in the western foothills of Taiwan are composed of soft sedimentary rocks, such as sandstone, siltstone, and shale, and covered with an armor layer of varying thickness. Due to low rock strength and head fall caused by the weirs, rapid scouring downstream of weirs is often observed once the armor layer is worn away. To evaluate weir stability, the shape and depth of scour holes must be identified. The scouring process assumed by existing approaches for estimating the depth of scour holes may not be applicable to weirs in Taiwan. Thus, field geology and scour investigations were conducted at eight sites of diversion weirs located in the western foothills of Taiwan. Based on collected data, three typical categories of

the scouring process downstream of weirs were identified. The suitability of existing approaches for calculating scour-hole depth on soft rock was also evaluated.

SCOURING PROCESSES DOWNSTREAM OF WEIRS

Rivers in Taiwan are typically short and steep. The slope of a river channel generally exceeds 1% in mountainous areas and 0.2–0.5% on plains. Taiwan receives on average roughly 2,500 mm of rainfall annually. Heavy rainfall for more than 1000mm/hour can occur during typhoons in summer. The runoff amount is also very high due to steep slopes and high rainfall intensity. For example, the watershed of the Chi-Chi Weir is about2,034 km^2, and maximum flow reaches 20,500 m^3/sec for a 100-year return period. As flow passes the weir, unit flow rate can reach 160 m^2/sec, and maximum flow velocity can be as high as 19 m/sec.

The western foothills of Taiwan contain relatively young rock formations, which have low resistance to weathering and erosion by water. Due to the high rainfall intensity, steep slope, and weak geology, the degree of weathering and erosion in watersheds in Taiwan is also very high. Moreover, landslides and debris flows caused by earthquakes and typhoons often occur, contributing to sedimentation of rivers. Monitoring data from the Water Resources Agency, Taiwan, show that the total sediment transport is 3.23 billon tons/year, and the unit sediment transport in many rivers can reach 10,600 tons/km^2, significantly higher than that of most rivers in other countries. These statistical data are also indicative of high river erosion potential in Taiwan.

To investigate scouring processes downstream of weirs, eight typical weirs in the western foothills of Taiwan were studied. Table 1 summarizes the basic data of these weirs. Except for the gravel armor at the Dong-Kou Weir, outcrop rocks at the other seven weir sites are sedimentary rocks. The armor layers at these weirs no longer exist, except for at the Dong-Kou Weir, where thick gravel deposits cover the underlying rock. At the Yi-Shing Weir, bedding planes and two sets of joints are well developed. All outcrops at other weir sites have clear bedding planes without clear joints. Based on the uniaxial compression strength of rock materials, the outcrop rock at the Yi-Shing Weir site can be classified as hard rock; all outcrop rocks at other weir sites are soft rocks. The strike of the rock strata with respect to the flow direction is roughly divided into the following two categories: (1) parallel, which is when the angle between the strike and flow is <45°; and, (2) perpendicular, which

when the angle between the strike and flow is >45°. Flow conditions around scour holes observed in the field are similar to those observed by Lin (2001) in flume tests.

Based on field geology data, site investigations, and erosion patterns of the eight weirs, three categories of scouring processes downstream of weirs were identified, namely, (1) plucking, (2) uniform incision, and (3) trenching incision. These categories are described as follows.

Table 1. Basic data of the studied weirs

Weir Name	Starting time of operation	Height (m)	Length (m)	Geomaterial*	UCS** (MPa)	Orientation.
Yi-Sing	1973	25.5	100	Ss	70-100	parallel
Hou-Chun	1983	3	556.3	Ss, Sh	10-20	parallel
Shih-kang	1977	21.4	240	Ss, Sh	2-12	parallel
Chi-Chi	2001	15	352.5	Ss.&Sh	5-15	parallel
Long-Quan	1982	3	80	Sh	2-30	perpendicular
Chu-Kou	1999	1.5	72	St with sh	5-10	perpendicular
Gia-Sian	1999	7	120	Sh	10-25	perpendicular
Dong-Kou	1973	5	220.8	Gravel	-	-

*Ss = sandstone; Sh = shale; Ss.&Sh = alternating layers of sandstone and shale.; St: Siltstone.

**UCS: Uniaxial compression strength

(1) Plucking:

The plucking scouring process was observed at the Yi-Sing Weir. This weir is constructed on meta-sandstone with uniaxial compression strength of 70–100 MPa. The outcrop rock has clear bedding planes and two sets of joints. Rock blocks formed by discontinuities exist at this site. Due to the high strength of the sandstone, the rock has high resistance to abrasion. Therefore, plucking of jointed rocks dominates scouring processes. A plunging pool formed due to falling water and blocky rock conditions (Figure 1(a)). Figure 1(b) presents the scouring processes and the shape of the scour hole. This process is similar to that discussed by Bollaert and Schleiss (2003). However, the scour hole appears asymmetrical; the slope in the upstream is gentler than that in the downstream. This differs markedly from that for dams built on hard rocks. Site inspection indicates that scouring depth under the weir foundation was about 7 m. Engineering countermeasures was initiated to mitigate this instability.

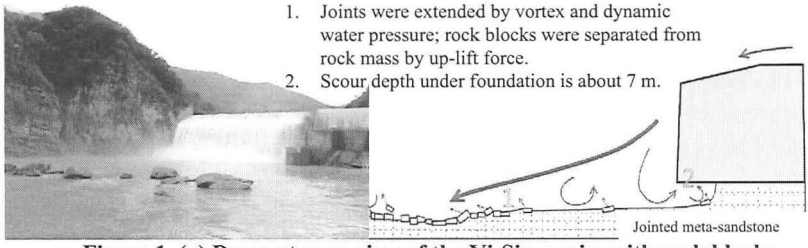

Figure 1. (a) Down-stream view of the Yi-Sing weir: with rock blocks mounding at Down-stream of scour hole. (b) Illustration of the plucking type of scouring processes.

(2) Uniform Incision:

The uniform incision scouring process exists at the Long-Quan Weir, Chu-Kou Weir, and Gia-Sian Weir. The rocks at these sites are composed of massive soft sandstone, massive shale, or massive siltstone with thin shale layers. The flow direction is perpendicular to the strike of beddings. Due to the low rock strength and very few joints, abrasion of massive rocks dominates the scouring process. The strength of the soft rock is isotropic; thus, rock abrasion by the flow vortex induced by a jet remains uniform and a circular scour hole is gradually formed. Since the jet impinges a relatively small incline angle relative to the horizontal plane, the slope of scour hole in the upstream is gentler than that in the downstream, which is similar to the case of category 1 (*i.e.,* plucking). If a flow contains large-grain sediments, the scouring rate downstream of weirs increases. Fractures may also develop on rock surfaces when granular sediment impacts rocks. Small-scale plucking scouring may then occur. Figure 2 shows a photograph of the area downstream of the Long-Quan Weir, illustrating the uniform incision scouring process.

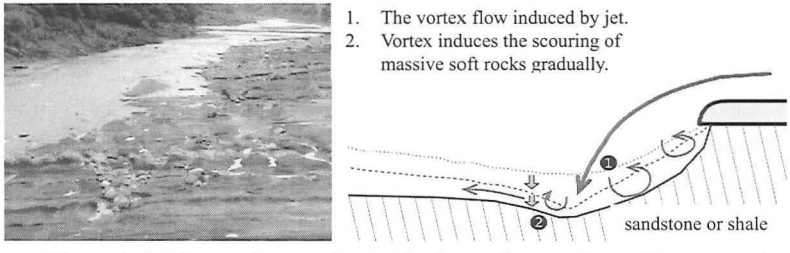

Figure 2. (a) Down-stream view to the Long-Quan weir: uniform scouring process. (b) Illustration of the uniform incision type of scouring process.

(3) Trenching Incision:

Trenching incision exists at the Hou-Chun Weir, Shih-kang Weir, and Chi-Chi Weir. Figure 3 shows a photograph downstream of the Hou-Chun Weir, illustrating the cross section perpendicular to flow of the trenching incision scouring process. The rocks at these sites are composed of alternating layers of massive sandstone and thin layers of shale, or alternating layers of massive shale and massive sandstone. The flow direction is parallel to the strike of beddings. Both sandstone and shale are soft rocks. Since the strength and erodibility of alternating thin layers of shale and sandstone is lower than that of massive sandstone, differential abrasion occurs at different layers. The alternating thin layers with low abrasion resistance are eroded faster and flutes at weak layers will develop along the flow direction. Subsequently, fractures developed in massive sandstone due to pressure relief. If rock blocks impact flutes via vortex or flow, the scouring rate increases. Over the long term, a trench along the strike developed.

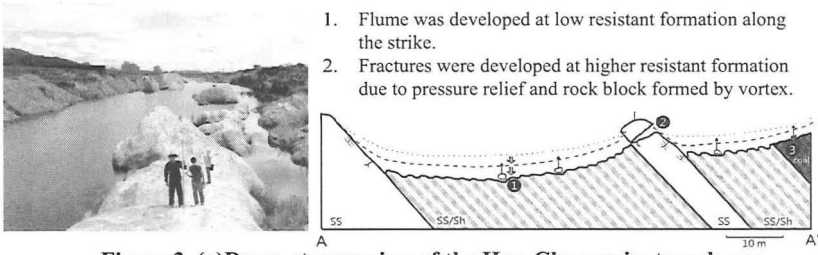

Figure 3. (a)Down-stream view of the Hou-Chun weir: trench was developed along the strike. (b) Illustration of the cross section perpendicular to flow: the Trenching incision type of scouring process.

EVALUATION OF SCOUR-HOLE DEPTH

The depths of scour holes evaluated by the methods developed by Annandale, *et al.* and Bollaert and Schleiss were compared with observed data for the Yi-Sin and Chi-Chi weirs to evaluate the suitability of these methods. The two-dimensional numerical program CCHE2D was utilized to calculate hydraulic conditions adjacent to weirs. The CCHE2D model is based on the efficient element method and used the implicit scheme by time stepping to solve continuity equations in each grid (WRA, 2009). Flow rates were chosen for different returning periods. Based on erodibility indices evaluated in field, scour depths at the Chi-Chi and Yi-Sin weirs were

calculated using the Annandale headcut model and the model developed by Bollaert and Schleiss (2003).

For a known erodibility index, erosion resistance in terms of stream power can be estimated using the Annandale headcut model. Compared with calculated erosive stream power for various elevations of rock beds, one can determine a scour depth at which erosive power is less than erosion resistance in terms of stream power. Using the model developed by Bollaert and Schleiss (2003), scour depth can be estimated based on force equilibrium of rock blocks; the size of a rock block that can be removed by an uplift force can be evaluated, such that scour-hole depth can be estimated. The erodibility index at the Chi-Chi Weir and Yi-Sing Weir was about 600 and 2000, respectively.

Based on field observations, notable rock scouring occurred at the Chi-Chi Weir during Typhoon Kalmaegi in 2008, which discharged 10,900 m^3/s of water flow, corresponding to a return period exceeding 2 years. In this event, a 3-meter scour depth was observed downstream of the Chi-Chi Weir. The scour hole at the Yi-Sing Weir was 15 m deep and had not yet stabilized. During 2001–2008, this scour hole deepened to 6.2 m, resulted from a maximum discharge of up to 8,527 m^3/s.

Table 2 compares actual and estimated scour-hole depths downstream of the two weirs. The estimated depth of the scour hole at the Chi-Chi Weir by the Annandale model is close to the actual magnitude, but the estimated depth significantly underestimates the magnitude of the scour hole at the Yi-Sing Weir. Conversely, the Bollaert-Schleiss model predicted a similar scour-hole depth at the Yi-Sing Weir, but largely overestimated that at the Chi-Chi Weir. This large difference may be attributed to (1) different mechanical behaviors of soft rock compared to that of brittle rock, (2) different water-jet conditions, and (3) different scouring processes.

Both models were only partially successful and are not generally applicable. The applicability and limitations of both methods warrant further examination.

Table 2 The actual and estimated scouring depths.

Scouring Depth	Actual	Estimated by Annandale model	Estimated by Bollaert-Schleiss model
Chi-Chi weir	3 m	~3 m	23 m
Yi-Sing weir	15 m	1.5 m	>15 m

CONCLUSIONS

Based on data from field geology investigation, site investigations, and scouring pattern recognition for the eight weirs, this study identified three typical categories of scouring process downstream of weirs, namely, (1) plucking, (2) uniform incision, and (3) trenching incision. The plucking scouring process is the dominant process for weirs constructed on jointed hard rocks. The other two processes typical in areas with soft rock. Furthermore, the factors influencing the types of scouring processes were identified; these factors include the type and properties of geo-materials, attitude of discontinuities, density and spacing of discontinuities, and flow conditions. Due to differences in flow conditions, the observed shape of scour holes downstream of weirs, especially for weirs built on soft rocks, differs from that of scour holes downstream of high dams. The scour hole appears asymmetrical; the slope in the upstream is gentler than that in the downstream.

To evaluate the suitability of existing approaches for calculating scour-hole depth on soft rock, the approaches developed by Annandale *et al.* and Bollaert and Schleiss were used to calculate scour-hole depth at two sites. We conclude that both these methods are only partially successful and are not generally applicable to scouring downstream of a weir on a soft-rock riverbed. This may be attributed to (1) different mechanical behaviors of soft rock, (2) different water-jet conditions, and (3) different scouring processes. Based on the real scouring processes for soft rocks, appropriate methods for scouring evaluation of soft rock, especially for local scouring downstream of a weir, warrant further study.

ACKNOWLEDGMENT

The authors would like to thank the Water Resources Agency and the National Science Council of the Republic of China, Taiwan, for financially supporting this research.

REFERENCES

Annandale, G.W. (1995). "Erodibility" *Journal of Hydraulic Research*. 33(4): 471-494.

Annandale, G.W. (2006). "Scour technology" McGraw-Hill, New York. 430p

Bollaert, E. and Schleiss, A. (2003). "Scour of rock due to the impact of

plunging high velocity jets Part I: A state-of-the art review" *Journal of Hydraulic Research*. 41(5): 451-464.

Bormann, E and Julien, P.Y. (1991). "Scour downstream of grade-control structures *Journal of Hydraulic Engineering, ASCE*, 117(5): 579-594.

Fahlbusch, F. E. (1994), "scour on rock riverbeds downstream of large dams" , Hydropower & Dams, pp.30-32.

Lin, C. (2001)."Prevention of scourng by overflow water or Hydraulic jump in bridge foundation" *Proc. Of Conference of Hydraulic Engineering*. 202-231 (in Chinese).

Liu ,P .Q. (2005). "A new method for calculating depth of scour pit caused by overflow water jets" *Journal of Hydraulic Research.* 43(6); 696-701.

Martins, R. (2006). "Contribution to the knowledge on the scour action of free jets on rocky river beds" *Proc. the 11th Congress on Large Dams*, Madrid, 799-814.

Schoklitsch, A. (1932)." Kolkbildung unter Überfallstrahlen. Die Wasserwirtschart", 341p.

Water Resources Agency. (2009). "A study on the mechanisms and evaluation of rockbed erosion after weir installation (1/2)" (in Chinese).

Whipple, K.X., Snyder, N.P. and Dollenmayer, K. (2000). "Rate and processes of bedrock incision by the upper Ukak river since the 1912 Novarupta ash flow in the valley of Ten Thousand Smokes, Alaska" *Geology.* 28(9): 835-838.

Hydraulic Loading for Bridges Founded on Rock

Su K. Mishra[1] M. ASCE, Ph.D., P.E., Jeffrey R. Keaton[2] F. ASCE, Ph.D., P.E., Paul E. Clopper[3] M. ASCE, P.E., and Peter F. Lagasse[4] F. ASCE, Ph.D., P.E.

[1] Senior Technical Advisor, HDR, 2365 Iron Point Road, Suite 300, Folsom, CA 95630; PH (916) 817-4860; email: su.mishra@hdrinc.com
[2] Senior Principal Engineering Geologist, MACTEC, 5628 East Slauson Avenue, Los Angeles, CA 90040, jrkeaton@mactec.com
[3] Senior Hydraulic Engineer, Ayres Associates, 3665 JFK Parkway, Suite 200, Fort Collins, CO 80525, clopperp@ayresassociates.com
[4] Senior Vice President, Ayres Associates, 3665 JFK Parkway, Suite 200, Fort Collins, CO 80525, lagassep@ayresassociates.com

ABSTRACT

Instantaneous stream power is defined as the product of shear stress and stream velocity representing the scouring condition. Hydraulic loading conditions are being expressed in terms of stream power which can be accumulated over the life of a bridge structure. The prediction of scour in erodible rock must consider the hydraulic loading imposed over many years over all the flood events over those years. This is true whether or not a threshold condition must be exceeded before the rock in the streambed is exposed to erosive forces. Long-term observations of scour in erodible rock combined with a history of hydraulic loading (expressed as stream power) provide a valuable index of the relative erodibility of the particular rock formation. An index, herein described as the Scour Number K_s, is defined as the amount of scour observed over a period of time divided by the cumulative hydraulic load over the same period. Given a future cumulative hydraulic loading, the Scour Number can be used to estimate the future scour associated with that loading, for the particular rock formation. Probability weighted flood frequency captures the range of flow conditions and is converted to average annual scour.

INTRODUCTION

The failure of the Interstate Highway 90 (I-90) Bridge over Schoharie Creek in New York during a flood in 1987 resulted in a Federal Highway Administration mandate for all bridges over water to be evaluated for scour susceptibility. Evaluating Scour at Bridges, Hydraulic Engineering Circular No. 18 (HEC-18; Richardson and Davis, 2001), has served the transportation community well for bridges founded on cohesionless, granular soils. HEC-18 procedures do not address cohesive soil or materials that are cemented or indurated (rock or rock-like formations). The I-90 Bridge over Schoharie Creek that failed in 1987 was founded on a glacial till formation that apparently was too hard to drive piles into when the bridge was constructed in 1954. Progressive scour from successive flood events undermined the spread footings but went undetected apparently because of an armoring layer of boulders and cobbles.

For short-term analysis like scour in non-cohesive material a single event such as the 100-year flood is typically selected for design purposes. However, scour in

rock is a process that must be considered over the long term (e.g., the remaining service life of the bridge). For a long-term approach, the objective is to evaluate the cumulative effects of a range of flow conditions. Therefore, a probability-weighted approach originally developed by Lagasse et al. (1985) to estimate average annual sediment yield using recurrence-interval events was adapted for use in predicting an equivalent average annual depth of scour in erodible rock. The method is straightforward in concept and simple to apply.

STREAM POWER

Power is defined as a rate of doing work or a rate of expending energy. In open channel flow, instantaneous stream power (the stream power at any particular moment) is defined as:

$$P = \gamma q S_f L = \gamma q(\Delta E) \tag{1}$$

where P = Instantaneous stream power, kW/m^2 (lb-ft/s per square foot)
γ = Unit weight of water, 9,800 N/m^3 (62.4 lb/ft^3)
q = Unit discharge, m^3/s per meter width (ft^3/s per foot width)
S_f = Slope of the energy grade line, m/m (ft/ft)
L = Unit distance in direction of flow, m (ft)
ΔE = Energy loss per unit distance in direction of flow

In terms of shear stress and velocity, Equation (1) may be rewritten as

$$P = \tau V \tag{2}$$

where τ = Representative shear stress, N/m^2 (lb/ft^2)
V = Representative velocity, m/s (ft/s)

The shear stress and velocity in Equation (2) must represent the conditions for which the scour is being evaluated. For example, if long-term scour across the entire cross section is of interest, the cross-sectional average velocity and bed shear will be satisfactory for use. However, if the scour at a specific location in the cross section is of interest, for example at a pier, then it is more appropriate to use local values for these variables. The maximum stream-tube velocity in the cross section V_{max}, multiplied by a shape factor K_p to account for local acceleration around the pier, will provide a more suitable representation of local conditions at the pier itself. Shape factors K_p are typically taken as 1.5 for round-nose piers and 1.7 for blunt (or square-nosed) piers, while the local shear stress is given as:

$$\tau = (nV)^2\left(\frac{\gamma}{y_0^{1/3}}\right) = \left(\frac{nV}{1.486}\right)^2\left(\frac{\gamma}{y_0^{1/3}}\right) \tag{3}$$

where τ = Local shear stress at the pier, N/m^2 (lb/ft^2)
n = Manning's n roughness coefficient

V	=	Local velocity ($K_p V_{max}$) at the pier, m/s (ft/s)
γ	=	Unit weight of water, 9,800 N/m^3 (62.4 lb/ft^3)
y_0	=	Depth of approach flow, m (ft)
1.486	=	Factor to convert English units to SI units

Substituting the expression for shear stress in Equation (3) into Equation (2) reveals that stream power is directly proportional to the cube of velocity. Therefore it is important that the location and magnitude of the representative velocity is selected with care. For example, computing stream power in the immediate vicinity of a square-nosed pier with a shape factor K_p of 1.7 will result in a stream power of $(1.7)^3 = 4.9$ times greater than the approach stream tube velocity just upstream of the pier.

INTEGRATED STREAM POWER

Integrated (or total) stream power, denoted Ω, is the area under the curve of stream power versus time for any particular flow duration, and is expressed in units of work (or energy loss) per unit area (kW-hr/m^2, lb-ft/ft^2). Using a time series of average daily flows typically obtained from USGS gaging station records, a time series of average daily stream power can be constructed as shown in Figure 1 which illustrates typical data from a single water year.

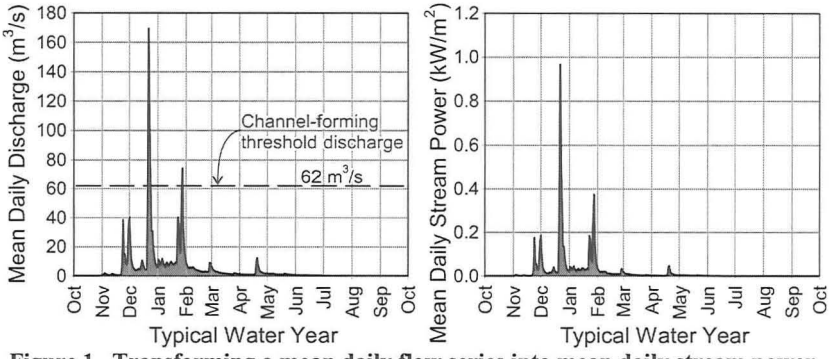

Figure 1. Transforming a mean daily flow series into mean daily stream power.

Integrated stream power shown in Figure 1 expressed in U.S. customary units is lb-ft/s/ft^2–day, since the time-base of the mean daily flow series is one day. Multiplying this value by 86,400 seconds per day gives lb-ft/ft^2, but the values themselves become cumbersome to work with; therefore, daily stream power is used.

THRESHOLD CONDITIONS

The physical processes involved in the scour of erodible rock may require that a threshold hydraulic condition be exceeded before scour can occur. Such thresholds could be, for example, a critical velocity, critical shear stress, critical stream power, or a geomorphic indicator such as a bank-full or "channel-forming" discharge. This can be an important process in many streams where relatively thin layers of gravel or cobbles overlie the rock in the streambed. These coarse bed materials must be

mobilized by a threshold hydraulic load before the underlying rock is exposed. Once the threshold is exceeded, however, the rock is exposed to the hydraulic forces of the flow, as well as to abrasion by the coarse bed materials that become mobile.

To illustrate this concept, consider the case where "effective" stream power is associated with a threshold value corresponding to a 2-year flood event, which is considered a channel-forming flow for a particular site. Flows less than the 2-year event therefore contribute no work towards eroding the rock of the streambed; however, once the 2-year value is reached or exceeded, the rock is exposed to the total stream power. The relationship between effective stream power and the threshold condition (in this case, discharge) is illustrated by Figure 2.

Using data from the time series shown in Figure 1, the graph of effective stream power vs. time is illustrated by Figure 3. Note in this figure that only two flood events in this particular water year exceeded the threshold condition, and active erosion of the rock (in this example) occurred over a total of only four days during the entire year. Both the daily series and the cumulative total stream power for the year are shown in this figure.

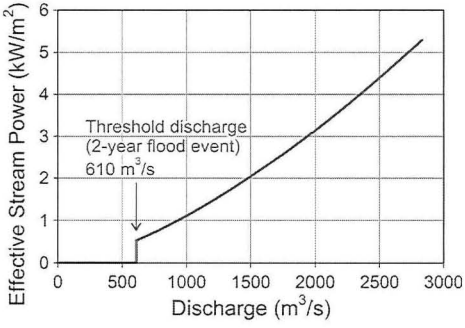

Figure 2. Effective stream power vs. discharge with a threshold condition.

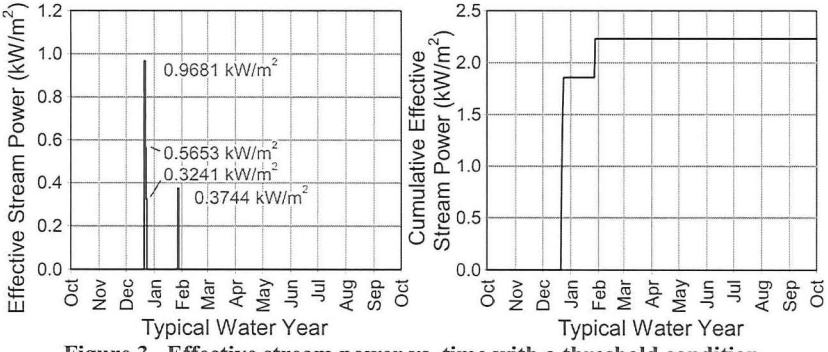

Figure 3. Effective stream power vs. time with a threshold condition.

Selection of a value for a threshold condition can be based or the caliber of bed load material protecting the rock channel or it can be based of geomorphic conditions, such as bankfull discharge. Geotechnical laboratory test results may be helpful in guiding selection of threshold hydraulic parameters for defining "effective" stream power. Additional research is needed on the stream-power threshold topic.

LONG-TERM CUMULATIVE STREAM POWER

The prediction of scour in erodible rock must consider the hydraulic loading imposed over many years by many flood events. This is true whether or not a threshold condition must be exceeded before the rock in the streambed is exposed to erosive forces. Consider the 71-year period of record of mean daily flows from 1938 to 2009 for the Sacramento River from USGS gaging station 11370500 at Keswick, California shown in Figure 4. For this reach, a 2-year event of 859 m^3/s is assumed to be the channel-forming discharge and will be used as a threshold condition to develop the long-term hydraulic loading (in terms of stream power) at this location.

State Route 273 crosses the Sacramento River near the Keswick gaging station. Comparison of survey data from January 1971 and November 2004 revealed that approximately 1.524 m of scour in the streambed rock (siltstone) in the vicinity of Piers 4, 5, and 6 had occurred over this period of time (approximately 33.8 years). From the graph of cumulative daily stream power for the Sacramento River at the SR 273 Bridge (Figure 5), the cumulative amount of effective daily stream power (i.e., contributed by events exceeding the 2-year discharge) in the 33.8 years between these two observations was approximately 336.5 kW/m^2.

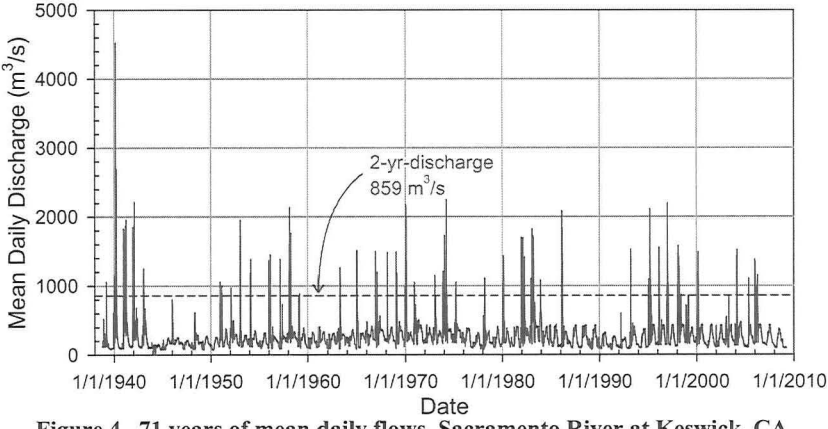

Figure 4. 71 years of mean daily flows, Sacramento River at Keswick, CA.

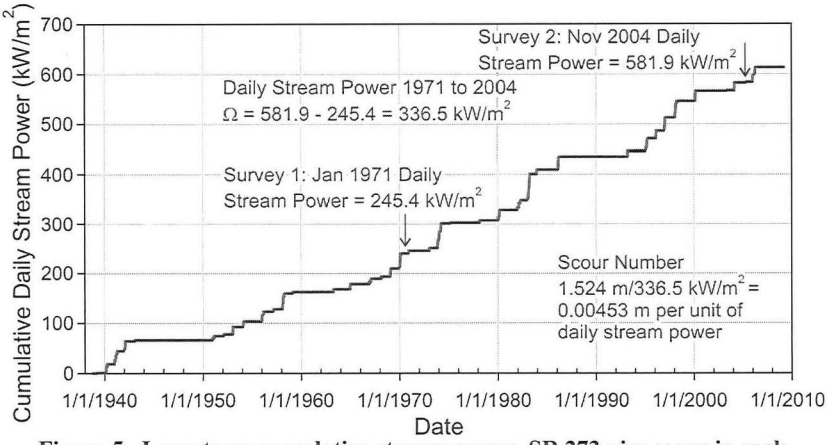

Figure 5. Long-term cumulative stream power, SR 273 pier scour in rock.

Long-term observations of scour in erodible rock combined with a history of hydraulic loading (expressed as stream power) provide a valuable index of the relative erodibility of the particular rock formation. In the case of the SR 273 Bridge over the Sacramento River, 1.524 m of pier scour over a 33.8-year period can be related to a cumulative hydraulic load over that same period of time. An index, herein described as the Scour Number K_s, is defined as the amount of scour observed over a period of time divided by the cumulative hydraulic load over the same period:

$$K_s = y_s / \Omega \tag{4}$$

where K_s = Scour Number, m (ft) per unit of effective stream power
y_s = Observed scour, m (ft) over a period of time
Ω = Cumulative effective daily stream power over the same period of time as the observed scour

Given a future cumulative daily hydraulic loading Ω_{fut}, the Scour Number can be used to estimate the future scour associated with that loading for the particular rock formation that was scoured to give the scour number. Estimates of future scour may then be made for a variety of purposes:

- Predicting scour over the remaining life of a structure
- Predicting scour at other existing structures with foundations in the same (or similar) rock formation
- Predicting scour at proposed structures on similar rock formations.

The difficulty with the above approach is estimating the cumulative effective hydraulic load in the future. Many rock scour issues are concerned with plucking or quarrying processes in durable, jointed rock for which a threshold condition applies; therefore, only the effects of larger, relatively infrequent events over the life of the structure need be considered. Scour in erodible rock is gradual and progressive, which lends itself to a process model known as the probability-weighting approach.

PROBABILITY-WEIGHTED APPROACH

Using either observed scour depths vs. cumulative stream power over time, or an erosion rate relationship based on rock properties, an erosion rate function for recurrence-interval flood events for a particular site is defined as

$$(y_s)_i = f(\Omega, t) \tag{5}$$

where $(y_s)_i$ = Scour depth associated with a flood of recurrence interval i, where i = 2, 5, 10, 25, 50, 100, or 500 years

Ω = Total stream power associated with the recurrence interval flood

t = Duration of the flood, days

The probability weighted approach accounts for the probability of occurrence of various flood events during any one year. For example, if $(y_s)_i$ is the scour associated with a given flood of recurrence interval i, and P_i is the annual probability that the given flood will occur, then the product $(y_s)_i \times P_i$ represents the contribution of that given flood to the long-term mean annual scour depth. To account for the contribution of all possible floods requires the integration

$$\bar{y}_s = \int_0^1 (y_s)_i \, dP_i \tag{6}$$

This integration is easily accomplished using the flood frequency curve. The frequency curve for scour associated with each recurrence-interval flood is developed by computing the scour using Equation (5). Figure 6 illustrates a typical scour-frequency curve. The area under the curve represents the mean annual scour depth, and can be computed either graphically or numerically. A simple approximation is a stepwise integration using Simpson's Rule as follows:

$$\begin{aligned}\bar{y}_s = {} & 0.002(y_s)_{500} + 0.008\left(\frac{(y_s)_{500} + (y_s)_{100}}{2}\right) + 0.01\left(\frac{(y_s)_{100} + (y_s)_{50}}{2}\right) + \\ & + 0.02\left(\frac{(y_s)_{50} + (y_s)_{25}}{2}\right) + 0.06\left(\frac{(y_s)_{25} + (y_s)_{10}}{2}\right) + 0.1\left(\frac{(y_s)_{10} + (y_s)_5}{2}\right) + \\ & + 0.3\left(\frac{(y_s)_5 + (y_s)_2}{2}\right) + 0.5\left(\frac{(y_s)_2 + 0}{2}\right)\end{aligned} \tag{7}$$

Expanding Equation (7) and combining like terms, the estimated average annual scour can be simplified to:

$$\begin{aligned}\bar{y}_s = {} & 0.006(y_s)_{500} + 0.009(y_s)_{100} + 0.015(y_s)_{50} + 0.04(y_s)_{25} + \\ & + 0.08(y_s)_{10} + 0.2(y_s)_5 + 0.4(y_s)_2\end{aligned} \tag{8}$$

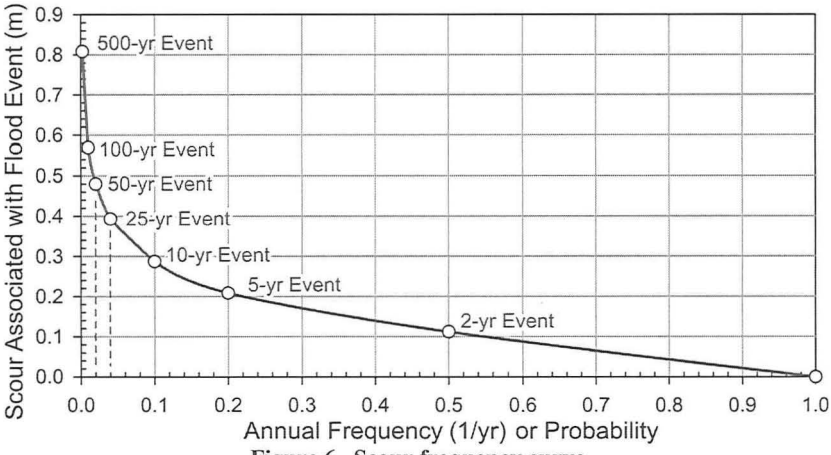

Figure 6. Scour frequency curve

The coefficients in Equation (8) clearly show that the scour contributions from larger, rare flood events are weighted less heavily than the scour from smaller, more frequent events. Thus, over the long term, the total scour at a bridge y_{max} during its remaining service life ΔT is estimated to be $y_{max} = (\bar{y}_s)(\Delta T)$. If one assumes that a threshold condition, for example the 2-year flood, must be exceeded before the hydraulic load (represented by stream power) can begin to erode the rock in the stream bed, the last term of Equations (7) and (8) may be neglected.

CONCLUSION

The method described in this paper was applied at bridge sites in New York (Schoharie Creek), California (Sacramento River), Florida (Chipola River), and Oregon (Mill Creek) as part of the research work for NCHRP Project No. 24-29. In each of the cases, the method proved to be a suitable procedure to predict long-term scour at bridges founded on rock-like material. The Scour Number K_s was used to predict the scour over a time period. In subsequent work on this project, samples of rock collected at the bridge sites were subjected to geotechnical testing. An equivalent geotechnical scour number, which is the representative erosion rate based on the response of rock fragments to energy dissipation, was developed which appears to be useful in predicting scour in degradable rock, even in the absence of historical hydraulic loading data. The geotechnical scour number is described by Keaton and Mishra (2010); it is appropriate for rock material that scours by grain-scale wear in response to hydraulic loading or abrasion. It is not appropriate for jointed durable rock that scours by quarrying and plucking of blocks defined of joint, fracture, or bedding planes, which is a threshold-controlled process. The geotechnical scour number has been calibrated at only one location: the SR 273 Bridge across the Sacramento River at Redding, California. It is a promising approach that deserves additional research.

ACKNOWLEDGMENTS

The research described in this paper is part of a National Cooperative Highway Research Program project to develop guidelines for evaluating scour at bridge foundations or rock (NCHRP Project 24-29). The first author of this paper is the co-principal investigator; he was a Senior Hydraulic Engineer with Ayres Associates during nearly all of the research.

REFERENCES

Keaton, J.R., and Mishra, S.K. (2010). Modified Slake Durability Test for Erodible Rock Material, *Proceedings 5th International Conference on Scour and Erosion* (this conference).

Lagasse, P.F., Schall, J.D., and Peterson, M. (1985). Erosion Risk Analysis for a Southwestern Arroyo, *Journal of Urban Planning and Development*, Vol. 111. No. 1.

Richardson, E.V., and Davis, S.R. (2001). Evaluating Scour at Bridges. *Hydrologic Engineering Circular 18*, Federal Highway Administration, 4th Edition, Publication No. NHI 01-001, 378 p.

Modified Slake Durability Test for Erodible Rock Material

Jeffrey R. Keaton[1] F.ASCE, Ph.D., P.E. and Su K. Mishra[2] M.ASCE, Ph.D., P.E.

[1]Senior Principal Engineering Geologist, MACTEC Engineering and Consulting, Inc., 5628 East Slauson Avenue, Los Angeles, CA 90040; PH (323) 889-5316; email: jrkeaton@mactec.com
[2]Senior Technical Advisor, HDR, 2365 Iron Point Road, Suite 300, Folsom, CA 95630; PH (916) 817-4860; email: su.mishra@hdrinc.com

ABSTRACT

The slake durability index (ASTM D4644-08) measures the response of rock fragments to submerged tumbling action. This test was modified to eliminate oven drying, extend test-increment duration, and increase the number of test increments to better reflect conditions in rock-bed stream channels. The results are expressed as a linear dimension taken to represent equivalent scour depth and normalized cumulative power taken to represent equivalent stream power. Sample loss during the first test increment is dominated by rounding of fragment edges and corners; hence, it is disregarded. Subsequent test increments display a linear trend, the slope of which is defined as the 'geotechnical scour number'. The geotechnical scour number of thinly bedded siltstone is similar to an 'empirical scour number' calculated from measured scour and cumulative stream power for the same location. Scour numbers for other rock types were consistent with observed channel behavior suggesting that the modified slake durability test may be valuable for predicting scour at bridge sites.

INTRODUCTION

Scour of earth materials characterized by cohesion, cementation, or induration is cumulative and progressive, unlike cohesionless, granular soils which respond rapidly to peak hydraulic loading. Procedures for evaluating scour of sand-bed channels (e.g., Richardson and Davis, 2001) have been available for some time, but procedures for rock-bed channels are being developed by the authors of this paper through National Cooperative Highway Research Program Project No. 24-29.

Four modes of rock scour exist: 1) dissolution of soluble rocks, 2) cavitation, 3) quarrying and plucking of durable blocky rocks, and 4) grain-scale wear of erodible rocks. The rock-scour mode addressed in this paper is the gradual, but progressive grain-scale wear of erodible rock material. The example presented in this paper pertains to the Sacramento River at Redding, Shasta County, California, USA.

The purpose of this paper is to describe modifications to a standard test procedure (the slake durability index) and its applicability to rock scour. The first application of the slake durability test to rock scour was done in Oregon by Dickenson and Baillie (1999). These researchers modified the standard procedure and produced an abrasion number to describe the response of the rocks to the submerged tumbling action. We were impressed by their modifications and applied them in our own research. Dickenson and Baillie (1999) used stream power to represent hydraulic loading. We also use stream power because it combines all hydraulic parameters and can be accumulated meaningfully. The importance of stream power became clear to

us during analysis of stream gage data, which led us to an 'empirical scour number'. This concept prompted us to express modified slake durability test results in equivalent stream power terms, which led us to a 'geotechnical scour number'.

SLAKE DURABILITY TEST

The slake durability index (ASTM D4644-08) is defined as "the percentage by dry mass of a collection of shale pieces retained on a 2.00 mm (No. 10) sieve after two cycles of oven drying and 10 minutes of soaking in water with a standard tumbling and abrasion action." The standard test calls for 10 roughly equidimensional fragments and a total specimen weight between 450 and 550 grams. The standard tumbling action is accomplished in a drum that rotates at 20 revolutions per minute. The standard drum is 100 mm long and 140 mm in diameter with sides composed of the 2-mm mesh. The lower approximately 40% of the drum is submerged in a water reservoir; the axis of rotation is approximately 15 mm above the water surface.

A slake durability index of 5.3 was determined for siltstone from the Sacramento River at Redding, California, using the ASTM D4644 procedure. This index value indicates that 94.7% of the sample passed through the No. 10 sieve mesh after oven drying and two 10-minute cycles of submerged tumbling.

ABRASION NUMBER

Dickenson and Baillie (1999) determined that conventional slake durability results were unrepresentative of conditions in western Oregon streambeds underlain by degradable rock formations because the channel bottoms were never completely dry. They eliminated oven drying and extended test cycles to 30 minutes for the first 2 hours, and 60 minutes for the next 7 hours. Dickenson and Baillie (1999) determined sample weights using the 'saturated surface dry' procedure (ASTM C127) and disregarded the first few readings because of corner and edge rounding. They defined the slope of percent loss versus natural log cumulative time as an 'abrasion number' and correlated the abrasion number with observed channel degradation and cumulative stream power from stream gage data to develop a predictive relation. Two samples of siltstone were evaluated using these procedures as shown on Figure 1. The average abrasion number is 17.9 for the two samples shown on Figure 1b.

SCOUR NUMBER

Empirical scour number

Relatively long-term scour can be determined from repeated cross sections. California Department of Transportation provided data for the Market Street Bridge (State Route 273) over the Sacramento River at Redding. These data indicated about 1.52 m (5 ft) of pier scour occurred on the upstream side of the bridge over a 33.8-yr period. Daily flow series from a nearby gage (USGS Gage 11370500 at Keswick) were used to calculate a cumulative stream power of 3.37e+5 W/m^2 (23,100 ft-$lb/s/ft^2$) during the same 33.8-yr period. We define the empirical scour number as the

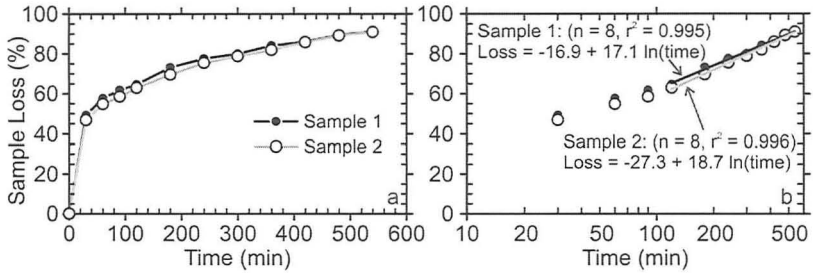

Figure 1. Slake durability results using the modification of Dickenson and Baillie (1999) for two samples of thinly bedded siltstone from the Sacramento River at Redding, Shasta County, California, USA. a. Arithmetic plot; b. Semi-log plot.

measured scour depth divided by stream power accumulated over the same period. An empirical scour number of 4.53e-6 m/W/m^2 (0.000217 ft/ft-lb/s/ft^2) was calculated for the Market Street Bridge.

Geotechnical scour number

We further modified the slake durability test to consist of 60-minute increments for 9 hours and expressed the results as equivalent scour depth and equivalent stream power. The results must be normalized to an initial weight to permit direct comparison of energy dissipation demonstrated by different samples; we used an initial weight of 500 grams, which is the midpoint of the total sample weight range in ASTM D4644. Equivalent scour depth was calculated by dividing the weight loss during a test increment by the unit weight of the rock material determined by ASTM Procedure C127 for concrete aggregate to produce a loss volume, which was normalized by unit area to give a linear dimension taken to be equivalent scour depth.

Equivalent power was calculated by multiplying the average sample weight during the test increment times equivalent distance traveled during the test increment, dividing the product by cycle duration in seconds, and normalizing the result by the area of the bottom 1/8 (45°) of the test drum. The equivalent distance traveled is the circumference of the drum times the rate of rotation times the duration of the test increment. The normalizing area is arbitrary, but corresponds to the area of residence of the sample fragments during the test. Average sample weight times distance traveled is energy (1 N-m = 1 J); energy per unit of time is energy dissipation or accumulation, which is power (1 J/s = 1 W). Power per unit area matches the units of conventional stream power calculated as the product of hydraulic shear stress (N/m^2 or lb/ft^2) and flow velocity (m/s or ft/s), for example 1 N-m/s/m^2 = 1 W/m^2.

The results of the modified slake durability test on the siltstone from the Market Street Bridge are plotted on Figure 2. The data plotted on Figure 1 represent the same tests on siltstone, but the 30-minute increment data were not used on Figure 2. The initial data points have the highest equivalent scour depth and equivalent stream power because sample fragments are being rounded and the sample

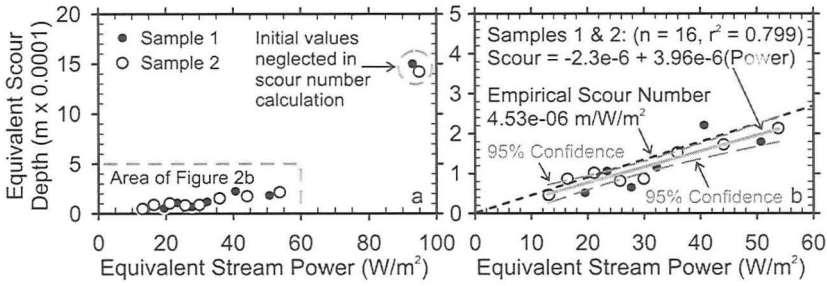

Figure 2. Modified slake durability results for two samples of thinly bedded siltstone from the Sacramento River at Redding, Shasta County, California, USA. Regression line slope on Figure 2b is the geotechnical scour number. Dashed line on Figure 2b is the empirical scour number.

weight is the largest at any point during the test. The slope of equivalent scour depth versus equivalent stream power is defined as the 'geotechnical scour number'. The siltstone data from Figure 1 produced a geotechnical scour number of 3.96e-6 m/W/m^2 (0.00019 ft/ft-lb/s/ft^2). The empirical scour number (4.53e-06 m/W/m^2) is nearly within the 95% confidence interval of the regression, as shown on Figure 2b.

Geotechnical scour numbers for claystone, limestone, blocky siltstone, and sandstone were measured using the same procedure (Figure 3). The results were consistent with observed channel behavior suggesting that the modified slake durability test may be valuable for bridge scour evaluations. The geotechnical scour numbers in this paper were calculated for sedimentary rock types. We believe that the geotechnical scour number may represent a basic characteristic of earth materials that are cemented or indurated; it also may be a useful characteristic of cohesive soils.

DISCUSSION AND CONCLUSIONS

The oven drying component of the slake durability test induces rapid slaking in susceptible materials that is unrepresentative of most rock-bed channel conditions; therefore, it is sensible to eliminate oven drying from the ASTM D4644 procedure. The abrasion numbers of the two samples shown on Figure 1b are nearly identical and represent the time-rate of material loss in response to the standard tumbling action of the slake durability test.

The slake durability test involves a standard drum rotating at 20 rpm. This combination of drum dimensions and rate of rotation produces an equivalent sample velocity of 0.147 m/s (0.481 ft/s). We considered plotting abrasion number as a function of equivalent sample velocity. We realized that modifying the rate of rotation of the slake durability drum would be needed to produce several equivalent velocities against which to evaluate sample response. We also realized that the equivalent energy was a function of the sample size, and that energy dissipated during test increments as the sample size diminished. Since we were representing hydraulic loading in terms of cumulative stream power, it was logical to represent the results of the modified slake durability test in equivalent stream-power terms.

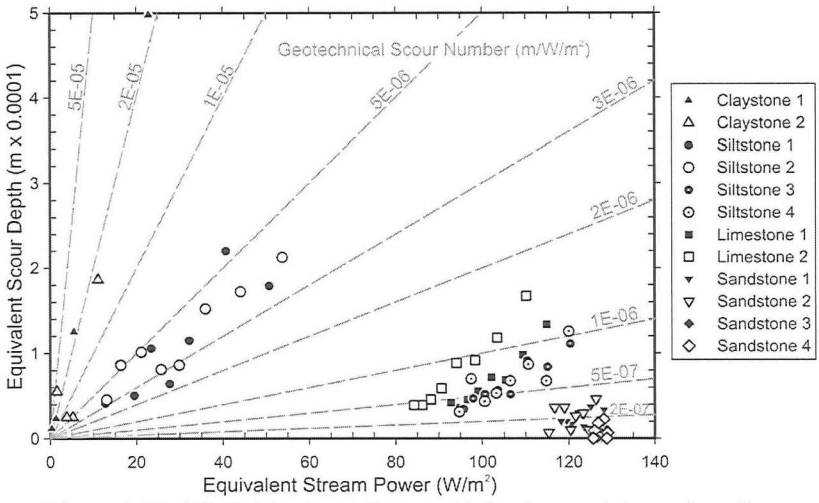

Figure 3. Modified slake durability results for four rock types from five locations. Claystone from San Juan County, Utah; thinly bedded siltstone from Shasta County, California (Siltstone 1 and 2; also in Figure 2); blocky siltstone from Polk County, Oregon; limestone from Jackson County, Florida; sandstone from San Juan County, Utah (Sandstone 1 and 2); sandstone from Montgomery County, New York. Dashed lines represent scour numbers in m/W/m^2.

Geotechnical scour numbers are not correlatable with the headcut erodibility index (NRCS, 2001) or the erodibility index method (Annandale, 2006). Geotechnical scour numbers are rates of rock material wear as a function of energy dissipation expressed as equivalent stream power accumulated over a period of time. The two index methods use threshold values to compare properties of earth materials (soil and rock) to peak discharge expressed as stream power. The threshold approach also is used by Richardson and Davis (2001) for evaluating scour of sand-bed channels at bridge openings. Threshold approaches imply that scour does not occur at all at flow conditions less than the threshold and that scour holes develop rapidly after the threshold is reached or exceeded. Peak velocity is used as the threshold hydraulic parameter for sand-bed channels (Richardson and Davis, 2001), whereas peak stream power is used as the threshold hydraulic parameter for rock-bed channels (NRCS, 2001; Annandale, 2006). Furthermore, the headcut erodibility index is not suited for channels without overfalls (NRCS, 2001, p. 32).

The erodibility index method uses stream power for turbulent flow in the near-bed region (Annandale, 2006, p. 121-141) rather than conventional stream power as the product of hydraulic shear stress and flow velocity. Available stream power with depth into a scour hole is calculated on the basis of the maximum possible scour depth using earth material with negligible scour resistance and the procedures described in Richardson and Davis (2001) to estimate the maximum possible scour depth (Annandale, 2006, p. 256-257). The erodibility index method predicts the depth

of scour as the depth at which the available stream power decreasing into the scour hole equals the equivalent resisting stream power of the earth material of the channel with the understanding that the ultimate scour hole can develop during a single discharge event if the threshold stream power is exceeded. Similarly, no scour occurs if the threshold stream power is not exceeded. The erodibility index value of the siltstone from the Sacramento River at Redding, CA, represented in Figures 1 and 2 is 0.1555 resulting in a threshold stream power of 0.2476 kW/m^2. The calculated applied stream power is 0.1989 kW/m^2. Thus, no scour would be predicted by the erodibility index method even though 1.52 m (5 ft) of pier scour was measured over a period of 33.8 years.

ACKNOWLEDGMENTS

The research described in this paper is part of a National Cooperative Highway Research Program project to develop guidelines for evaluating scour at bridge foundations or rock (NCHRP Project 24-29). The authors are grateful for review comments provided by Fred Kulhawy and Paul Santi, as well as by anonymous reviewers.

REFERENCES

Annandale, G.W. (2006). *Scour Technology*. McGraw-Hill, New York

ASTM. (2007). Standard Test Method for Density, Relative Density (Specific Gravity), and Absorption of Coarse Aggregate: *ASTM Standard C127*. American Society for Testing and Materials. ASTM International, West Conshohocken, PA (www.astm.org).

ASTM. (2008). Standard Test Method for Slake Durability of Shales and Similar Weak Rocks: *ASTM Standard D4644*. American Society for Testing and Materials, ASTM International, West Conshohocken, PA (www.astm.org).

Dickenson, S.E., and Baillie, M.W. (1999). Predicting Scour in Weak Rock of the Oregon Coast Range. *Unpublished research report,* Department of Civil, Construction, and Environmental Engineering, Oregon State University, Corvallis, OR. *Final Report SPR 382,* Oregon Department of Transportation and Report No. FHWA-OR-RD-00-04.

NRCS. (2001). Field Procedures Guide for the Headcut Erodibility Index: Chapter 52, Part 628, *National Engineering Handbook*, U.S. Department of Agriculture Natural Resources Conservation Service, 210-VI-NEH, rev, 37 p.

Richardson, E.V., and Davis, S.R. (2001). Evaluating Scour at Bridges. *Hydrologic Engineering Circular 18*, Federal Highway Administration, 4th Edition, Publication No. NHI 01-001, 378 p.

Scour at Bridge Foundations on Rock: Overview of NCHRP Project No. 24-29

Jeffrey R. Keaton[1] F.ASCE, Ph.D., P.E., Su K. Mishra[2] M.ASCE, Ph.D., P.E., and Paul E. Clopper[3] M.ASCE, P.E.

[1]Senior Principal Engineering Geologist, MACTEC Engineering and Consulting, Inc., 5628 East Slauson Avenue, Los Angeles, CA 90040; PH (323) 889-5316; email: jrkeaton@mactec.com

[2]Senior Technical Advisor, HDR, 2365 Iron Point Road, Suite 300, Folsom, CA 95630; PH (916) 817-4860; email: su.mishra@hdrinc.com

[3]Senior Hydraulic Engineer, Ayres Associates, 3665JFK Parkway, Building 200, Suite 200, Fort Collins, CO 80525; PH (970) 223-5556; email: clopperp@ayresassociates.com

ABSTRACT

National Cooperative Highway Research Program Project 24-29 focuses on time-rate and design depth of scour at bridge foundations on rock. Rock scour is related to five processes: 1) weathering, 2) dissolution, 3) cavitation, 4) plucking, and 5) abrasion. Guidance is provided for identifying scour processes which deserve evaluation. Quarrying and plucking is a threshold process governed by flow velocity, turbulence intensity and block size. Degradable rock scour is cumulative and expressed in terms of stream power which can be accumulated over time. Probability weighted flood frequency captures the range of flow conditions and is converted to average annual scour. Empirical scour number is defined as documented scour divided by cumulative stream power. Geotechnical scour number is calculated from modified slake durability test results. Design scour depth is probability weighted average annual scour times the remaining bridge life or cumulative stream power over a bridge life times the appropriate scour number.

INTRODUCTION

The goals of National Cooperative Highway Research Program (NCHRP) Project No. 24-29 are time-rate of scour and design scour depth at bridge foundations on rock. The guidance from this project will be integrated with Federal Highway Administration Hydraulic Engineering Circular HEC-18, Evaluating Scour at Bridges (Richardson and Davis, 2001). Bridge sites in Florida, Oregon, New York, Utah, and California visited in 2008 provided a range of data and samples for the research. Rock scour modes are considered separately for quantitative scour estimates.

ROCK SCOUR MODES

Rock scour in natural channels is related to five processes: 1) physical and chemical weathering of exposed rock surfaces, 2) soluble rock dissolution, 3) cavitation, 4), durable rock quarrying and plucking, and 5) degradable rock abrasion. The time between flood events can prepare rock-bed channels for scour in subsequent

floods. Check-list guidance for determining which scour processes can be dismissed and which deserve evaluation is shown in Figure 1.

Dissolution

Rocks such as halite, sylvite, and anhydrite can dissolve in water in periods of time short enough to be relevant in engineering application. Such rocks typically hare poor load-bearing capacity and are identified during routine foundation investigations. Common soluble rocks suitable for bridge foundations, such as limestone and dolostone, do not dissolve in engineering time scales. Prehistoric dissolution features of relevance in the context of rock scour consist of solution cavities completely or partially filled with heterogeneous rock rubble in a soil matrix.

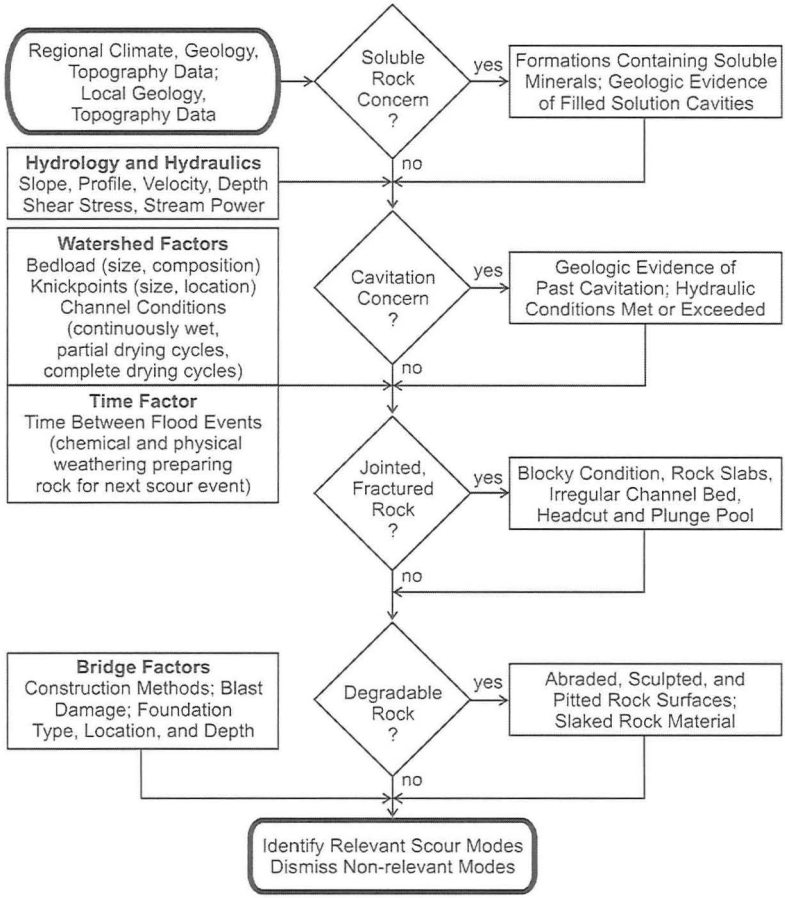

Figure 1. Rock-scour mode flow diagram.

Cavitation

Cavitation is an unstable condition in which water vapor forms bubbles that implode, releasing substantial energy. Cavitation can be relatively common in pipes and tunnels but not in natural channels. Water in natural channels rarely reaches the depth and velocity required for cavitation. Turbulence with entrained air mitigates the energy of imploding bubbles because the air is compressible. Mean flow depth and velocity conditions shown in Figure 2 defining likely and possible cavitation were derived from Barnes (1956), Baker and Costa (1987), and Whipple et al. (2000).

Plucking

Plucking of jointed rock blocks is a threshold process governed by turbulence intensity, flow velocity, and rock block size and geometry. Studies published in geomorphology literature built on flume experiments by Reinius (1986) and provided useful information for defining threshold flow velocities (e.g., Tinkler and Parish, 1998, Hancock et al., 1998). Numerical modeling of threshold flow velocities at bridge piers for rock block plucking and predicted scour depth relative to pier diameter was performed for this project by Bollaert (5th ICSE). An example of threshold velocities for plucking rock blocks is presented in Figure 3.

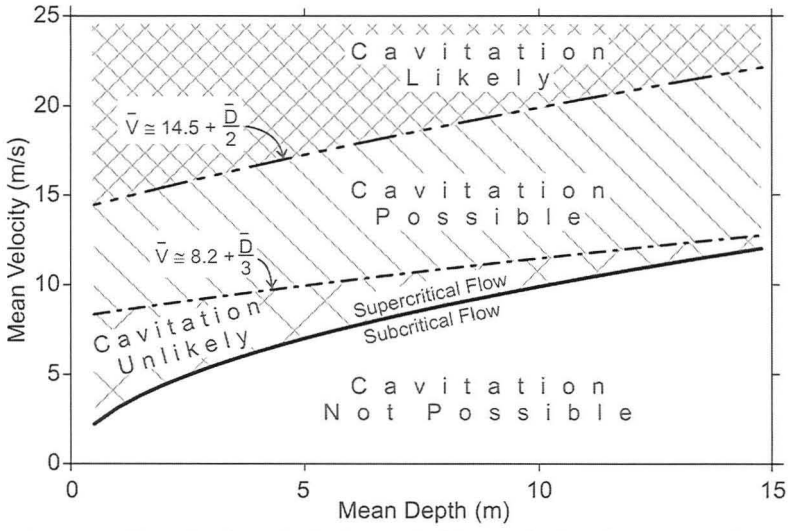

Figure 2. Flow depth and velocity needed for cavitation. Line separating subcritical and supercritical flow corresponds to a Froude number of 1.0. Linear equations on graph are approximate representations of the two curves.

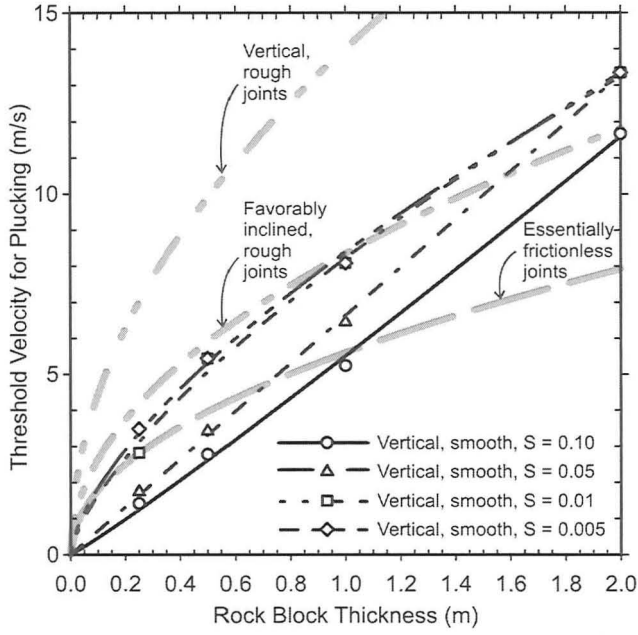

Figure 3. Threshold velocity required for plucking rock blocks. Essentially frictionless joints modified from Hancock et al. (1998); rough joints modified from Tinkler and Parish (1998). Data points and power-function regression curves calculated from data by Bollaert (5th ICSE); S denotes slope.

Abrasion

Abrasion is gradual and progressive, grain-scale erosion of degradable rock material in response to flowing water with or without saltating bedload. Hydraulic loading for degradable rock material is expressed as stream power (hydraulic shear stress × flow velocity = $[N/m^2] \times [m/s] = W/m^2$) because it incorporates all flow parameters and can be accumulated over time (Mishra et al., 5th ICSE). Cumulative stream power is calculated from daily flow series, including consideration of flow duration for various return period discharge events. Relatively long-term scour can be determined from repeated cross sections. Cumulative stream power is used to calculate an empirical scour number as the measured scour depth divided by the stream power accumulated over the same period. An example of an empirical scour number calculation for a bridge on the Sacramento River in Redding, CA, USA, is presented in Figure 4.

Equivalent scour depth and equivalent stream power are calculated from modified slake durability test (ASTM D4644) results (Keaton and Mishra, 5th ICSE). Equivalent scour depth is calculated from weight loss during a test increment divided by the rock material unit weight to produce a loss volume, which is normalized by unit area to give a linear dimension. Equivalent steam power is calculated by

multiplying the average sample weight during the test increment times equivalent distance traveled during the test increment, dividing the product by cycle duration in seconds, and normalizing the result by the area of the bottom 1/8 (45°) of the test drum where sample fragments reside during slake durability testing. The geotechnical scour number is equivalent scour depth divided by equivalent stream power. An example calculation is presented in Figure 5 for thinly bedded siltstone at the bridge on the Sacramento River in Redding, CA, USA, shown in Figure 4.

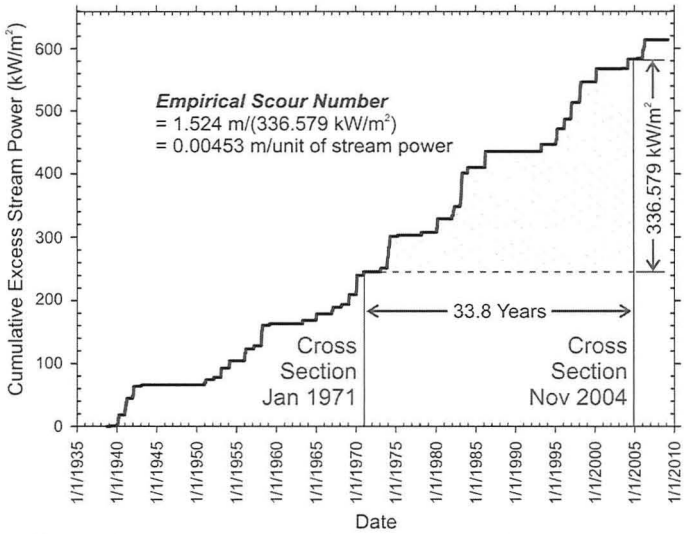

Figure 4. Empirical scour number calculation from daily stream power at the US Geological Survey Keswick gage on the Sacramento River at Redding produced by 2-year and larger discharge events. Cross sections on the upstream edge of a state highway bridge revealed 1.524 m (5 ft) of scour over 33.8 years.

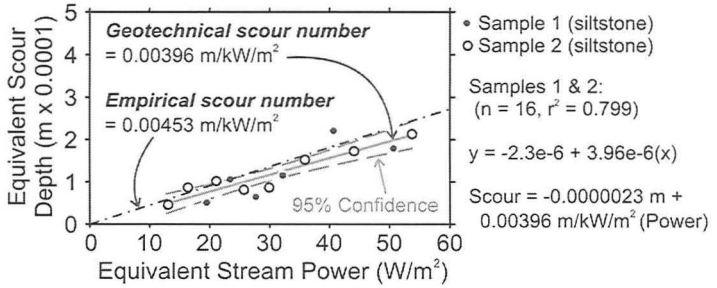

Figure 5. Geotechnical scour number calculation for siltstone samples from the bridge site in Figure 4. Empirical scour number from Figure 4 plotted for comparison.

SCOUR RATE AND DEPTH

The time-rate of scour is specific to different scour modes. Dissolution of soluble rocks in water occurs relatively slowly for rocks with suitable load-bearing capacity to support bridge structures. The scour rate of interest for soluble rocks would be governed by void-filling mixtures of rock fragments in a soil matrix too heterogeneous to be generalized. Scour rates in the soil matrix would govern the time-rate of scour. Rock blocks and fragments will collect in the scour hole if they are too large to be transported, thereby creating a natural armor condition on the channel bed and limiting the depth of scour.

Scour caused by threshold-controlled processes, such as cavitation or plucking, typically is assumed to develop to the maximum depth rapidly as soon as the threshold condition is exceeded. The depth of cavitation scour in natural channels has not been determined because cavitation is unstable and probably self-limiting by air entrainment and channel adjustments. The depth of plucking has been estimated by index methods (NRCS, 2001; Annandale, 2006) developed largely from empirical data collected in unlined spillway channels. Numerical modeling of threshold flow velocities for rock block plucking performed by Bollaert (5th ICSE) predicted scour depth relative to pier diameter; calibration of the model is needed for hydraulic conditions and geometries of natural channels.

Gradual and progressive scour of degradable rocks can be related to cumulative stream power and the empirical or geotechnical scour number. Flood frequency is calculated from daily flow series if gage data are available; otherwise, it can be estimated using conventional watershed relationships (Mishra et al., 5th ICSE). Flood event discharge is correlated to a cumulative excess stream power and then converted to scour depth by applying the empirical or geotechnical scour number. The inverse of flood return period is frequency; for example, the 2-year discharge corresponds to an average annual frequency of 0.5, whereas the 100-year discharge corresponds to an average annual frequency of 0.01. The area under the probability weighted flood frequency-scour depth curve is the average annual scour, as shown in Figure 6. The examples in Figure 6 consist of the Sacramento River at Redding, Shasta County, CA, and Schoharie Creek at the Interstate Highway 90 crossing in Montgomery County, NY. Shasta Dam on the Sacramento River was closed in 1945 and the discharge has been regulated since that time. Schoharie Creek is an unregulated watershed draining the north side of the Catskill Mountains.

Design scour depth is the product of the probability weighted average annual scour and the remaining life of a bridge structure or the product of cumulative stream power for the life of a bridge and the appropriate scour number. The amount of pier scour at the State Route 273 Bridge on the Sacramento River documented by California Department of Transportation over a 33.8-year period was 1.524 m (5 ft); the amount of scour calculated from the average annual scour at this location is 1.6 m (33.8 yr×0.048 m/yr from Figure 6). The amount of pier scour at the Interstate 90 Bridge on Schoharie Creek determined from forensic studies of the 1987 bridge failure (Resource Consultants and Colorado State University, 1987) was about 4.6 m (15 ft); the amount of scour calculated from the average annual scour at this bridge is 5.1 m (33 yr×0.155 m/yr from Figure 6).

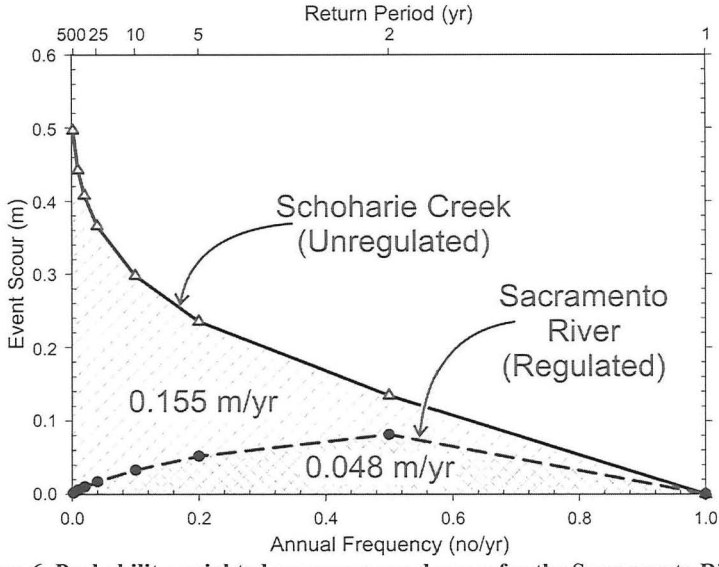

Figure 6. Probability weighted average annual scour for the Sacramento River, CA, and Schoharie Creek, NY. Sacramento River is regulated by Shasta Dam.

DISCUSSION AND CONCLUSIONS

Rock scour is a rock-water interaction phenomenon. Rock material ranges in properties from slightly better than good soil to much better than the best concrete. No rock material is resistant to the forces of water in the form of waterjets used to strip concrete away from reinforcing steel for bridge deck rehabilitation (Summers, 1995). In fact, waterjets can cut through the reinforcing steel if they are applied long enough. In natural, open channels, however, the stream power tends to be low enough that most rock materials can resist the hydraulic forces to some degree.

Soluble rock dissolution is not likely to be an important process at bridge sites because rocks that dissolve in engineering time have poor load-bearing capacity and would not be used for bridge support. Cavitation is not likely to be an important process at bridge sites because most natural channels cannot support the required hydraulic conditions or such channels would be spanned by bridges.

Durable rock plucking is analogous to scour of giant, interlocking sand grains. Threshold conditions characterized by hydraulic parameters at peak discharge control rock-block plucking similar to sand grains on sand-bed channels. Scour holes in sand-bed channels are thought to form rapidly as threshold conditions are reached; the holes are backfilled during waning stages of discharge with sand similar in character to the initial bed. Scour holes in rock-bed channels may be backfilled, but such backfill would not have the resistance of the initial rock-bed channel.

Degradable rock scour is gradual and cumulative. Threshold conditions probably exist, but scour holes develop in response to the applied hydraulic forces. The 100-year discharge may cause scour at a higher rate than the 2-year discharge,

but if the 100-year discharge duration is very small compared to the 2-year discharge duration, then the overall contribution to scour by the 100-year discharge would be much less than the 2-year discharge. The probability weighted average annual scour captures this concept. Index methods (NRCS, 2001; Annandale, 2006) applied to Sacramento River conditions show that the hydraulic loading is less than the scour resistance of the siltstone even though 1.5 m of scour has been documented.

REFERENCES

Annandale, G.W. (2006). *Scour Technology*, New York, McGraw-Hill, 430 p.

Baker, V.R., and Costa, J.E. (1987). Flood Power, in Mayer, L., and Nash, D., eds., *Catastrophic Flooding*, Boston, Allen & Unwin, p. 1-21.

Barnes, H.L. (1956). Cavitation as a Geological Agent *American Journal of Science*. v. 254, p. 493-505.

Bollaert, E.F.R. (2010). Numerical Modelling of Scour at Bridge Foundations of Rock, *Proceedings 5th International Conference on Scour and Erosion* (this conference).

Hancock, G.S., Anderson, R.S., and Whipple, K.X. (1998). Beyond Power: Bedrock Incision Process and Form, in Tinkler, K.J., and Wohl, E.E., eds., *Rivers Over Rock: Fluvial Processes in Bedrock Channels*, American Geophysical Union, Geophysical Monograph 107, p. 35-60.

Keaton, J.R., and Mishra, S.K. (2010). Modified Slake Durability Test for Erodible Rock Material, *Proceedings 5th International Conference on Scour and Erosion* (this conference).

Mishra, S.K., Keaton, J.R., Clopper, P.E., and Lagasse, P.F. (2010). Hydraulic Loading for Bridges Founded on Erodible Rock, *Proceedings 5th International Conference on Scour and Erosion* (this conference).

NRCS (2001). Field Procedures Guide for the Headcut Erodibility Index: Chapter 52, Part 628, *National Engineering Handbook*, U.S. Department of Agriculture Natural Resources Conservation Service, 210-VI-NEH, revol. 1, March, 37 p

Reinius, E. (1986). Rock Erosion, *Water Power & Dam Construction*, v. 38, p. 43-48.

Resource Consultants, Inc. and Colorado State University (1987). *Hydraulic, Erosion, and Channel Stability Analysis of the Schoharie Creek Bridge Failure, New York*, Consulting report prepared for National Transportation Safety Board and New York State Thruway Authority, paginated by section.

Richardson, E.V., and Davis, S.R. (2001). Evaluating Scour at Bridges. Hydrologic Engineering *Circular 18*, Federal Highway Administration, 4th Edition, Publication No. NHI 01-001, 378 p.

Summers, D.A. (1995), *Waterjetting Techology*, London, E & FN Spon, 616 p.

Tinkler, K.J, and Parish, J. (1998). Recent Adjustments to the Long Profile of Cooksville Creek, and Urbanized Bedrock Channel in Mississauga, Ontario, in Tinkler, K.J., and Wohl, E.E., eds., *Rivers Over Rock: Fluvial Processes in Bedrock Channels*, American Geophysical Union, Geophysical Monograph 107, p. 167 187.

Whipple, K.X., Hancock, G.S., and Anderson, R.S. (2000). River incision into bedrock: Mechanics and relative efficacy of plucking, abrasion, and cavitation *Geological Society of America Bulletin*. v. 112, no. 3, p. 490-503.

Bluestone Dam Rock Scour

M. F. George[1], PE and G.W. Annandale[2], D.Ing, PE, D.WRE

[1]Project Geological Engineer, Golder Associates Inc., Lakewood, CO 80227; PH: 303-980-0540; email: Michael_George@Golder.com

[2]Practice / Program Leader, Golder Associates Inc., Lakewood, CO 80227; PH: 303-980-0540; email: George_Annandale@Golder.com

ABSTRACT

Advancements in hydrologic methods have often yielded greater estimates for design flood events. This can be problematic for older dams when the constructed spillway can no longer adequately pass the revised flood estimate. Bluestone Dam is one such case where recent estimates have indicated more than a twofold increase in the design flood magnitude. Moveable bed physical hydraulic model studies for flows greater than the original design indicated complex flow conditions and the potential for significant scour in the unlined hydraulic jump stilling basin. The ability of the homogeneous gravel used in the model study to represent scour potential of intact rock in the actual basin was questionable. As such, Annandale's Erodibility Index Method was used to provide revised scour estimates within the stilling basin. This paper presents a unique solution to a complex problem.

Introduction & Background

Bluestone Dam is a concrete gravity dam located on the New River near Hinton, WV (USA). Built during the 1940's, the dam has a 241 m long spillway with 21 gated overflow spillway bays and 16 lower sluice gates. Flow from the spillway discharges into an unlined hydraulic jump stilling basin (Figure 1). A downstream weir controls the water level within the stilling basin, while baffles on the stilling basin apron and an end sill at the end of the apron are provided to dissipate energy and direct flow upwards before entering the basin. The dam also has six large penstocks (~ 6 m diameter) that can be opened to provide additional discharge capacity.

The spillway was originally designed to pass a probable maximum flood (PMF) event of 12,180 m^3/s while recent advancements in hydrologic methods, however, have indicated more than a twofold increase in the design flood magnitude to 28,320 m^3/s.

Local geology within the stilling basin consists of three main rock types: orthoquartzite, interbedded shale and orthoquartzite, and claystone.

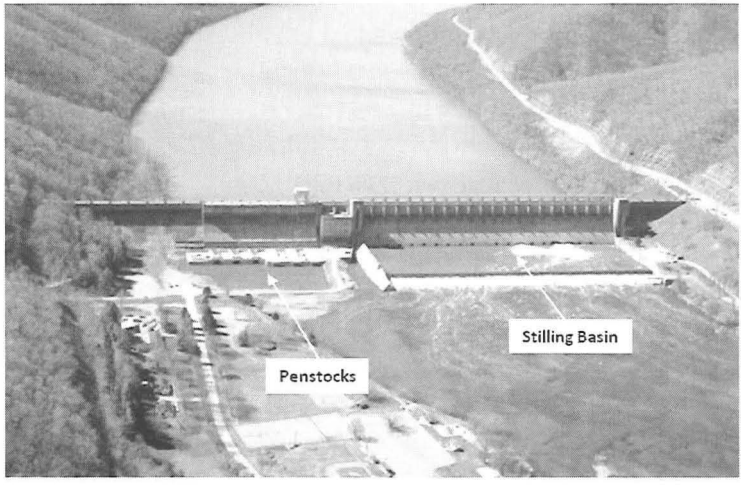

Figure 1. Bluestone Dam layout (Photo courtesy of USACE – Huntington District, Engineering Geology Section).

Physical Hydraulic Model Study

A 1:36 scale physical hydraulic model study was performed to examine scour potential from increased flows beyond the original design discharge up to the revised PMF of 28,320 m^3/s (USACE 2003b). A homogenous gravel bed, consisting of 1 cm size particles, was used to represent rock within the stilling basin.

Based on observation of the video taken of the physical hydraulic model, two main flow conditions exist over the range of discharges analyzed. For discharges up to the original design discharge, the basin functions as designed and a relatively well formed hydraulic jump is witnessed with little to no scour occurring. For the larger discharges, however, flow exiting the spillway into the basin closely resembles that of a "shooting jet". Comparison of the two scenarios is shown in Figure 2.

For the latter scenario, the end sill on the stilling basin apron directs flow upwards (similar to that of a flip bucket), causing the jet to skim on top of the tailwater in the basin and plunge downwards upon impact with the upstream face of the stilling basin weir. Scour-hole formation occurs on the upstream side of the stilling basin weir. Tailwater within the stilling basin is re-circulated forming a large eddy that transports scoured material in the downstream portion of the basin back towards the apron.

Results from the 1:36 scale model indicate a potential for up 27 m of scour within the basin under the revised PMF conditions, which would undoubtedly result in failure of the stilling basin weir. As using gravel to evaluate scour of intact rock in physical model studies may not be representative, it was desirable to attempt to determine how actual rock in the basin would influence scour.

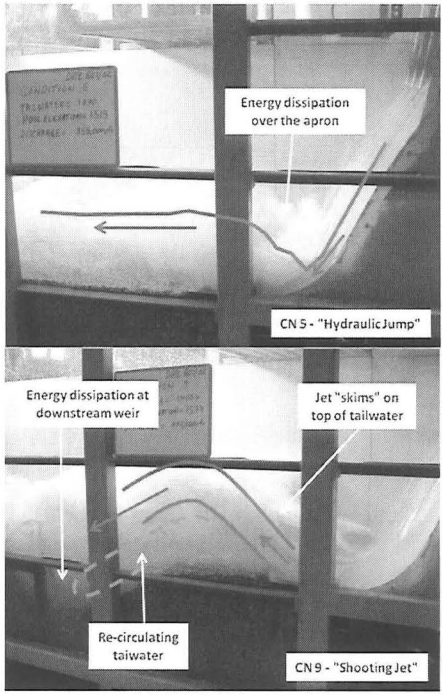

Figure 2. Comparison of flow conditions for discharges less than (top) and greater than (bottom) the original design discharge. Photos courtesy of USACE – Huntington District.

Calibration of Erosive Capacity

For discharges above the original design, flow conditions within the stilling basin are unique, and no one methodology can perfectly represent these conditions. As indicated in Figure 2, higher discharges loosely resemble a shooting jet and therefore jet and plunge pool theories were applied in an attempt to model these distinctive hydraulic conditions with known methods. Figure 3 shows a cross-section of the dam and stilling basin with a schematic of the plunging jet scour module as applied to Bluestone.

The methodology was modified by use of a calibration factor, applied to the calculation of flow erosive capacity within the stilling basin, to account for inadequacies of directly applying the plunging jet module to this flow scenario. Specifically this was done to account for 1) energy dissipation associated with flow through the baffle blocks on the basin apron, 2) the reduction in the jet flow rate applied to the stilling basin floor as an unknown portion of the jet is directed over the stilling basin weir, and 3) energy dissipation associated with jet impinging against the

back of the stilling basin weir and being re-directed downwards. The calibration factor was determined through the aid of the 1:36 scale physical hydraulic model.

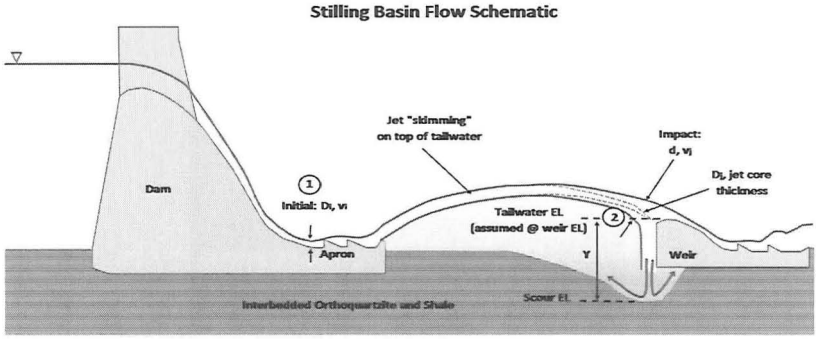

Figure 3. Schematic for shooting jet scenario showing applied plunge pool module (schematic based on typical section from USACE (2003a)).

For theoretical scour predictions, the erosive capacity of the plunging jet (expressed in units of stream power, W/m^2) could be calculated using Annandale's Erodibility Index Method (EIM) (1995, 2006):

$$P_{jet} = \frac{\gamma \cdot Q \cdot H}{A \cdot K} \cdot C_t$$

Where:
γ = unit weight of water (N/m^3).

Q = water discharge (m^3/s).

H = hydraulic head associated with the falling jet (m) taken between locations "1"and "2" on Figure 3.

A = impact area of the jet (i.e., jet footprint) (m^2).

K = factor to calibrate calculated erosive capacity to observed erosive capacity witnessed in the model study (see discussion below).

C_t = total dynamic pressure coefficient (dimensionless) used to determine the relative magnitude of erosive capacity as a function of tailwater depth. Although derived from pressure measurements, use of C_t to portray trends in erosive capacity within the plunge pool quantified by stream power has shown good promise (see George & Annandale 2006a, 2006b, 2008 and Lund et al. 2008). C_t can be expressed as:

$$C_t = C_p + RF \cdot \Gamma \cdot C_p^{'}$$

Where:

C_p = average dynamic pressure coefficient as a function of tailwater depth based on work by Castillo et al. (2007).

Γ = amplification factor to account for resonance that may occur in close-ended rock fissures as a function of tailwater depth (Bollaert 2002). Note that $\Gamma = 1$ (i.e., no amplification) for the calibration with physical model results (as the bed material is gravel) as well as for the theoretical scour calculations as characteristic frequencies for orthoquartzite and shale rock fissures were found not to be within the frequency range of major pressure fluctuations.

RF = unit reduction factor to account for influence of varying degrees of jet break-up based on work by Ervine et al. (1997).

$C`_p$ = fluctuating dynamic pressure coefficient as a function of tailwater depth based on work by Bollaert (2002).

To calibrate the calculated erosive capacity with the erosive capacity observed in the 1:36 scale physical hydraulic model, the calibration factor, K, was adjusted such that the theoretical scour depth matched the observed scour depth in model (Figure 4). Doing so required knowledge of the prototype erosion resistance of the gravel used in the physical model. This is discussed in the following section.

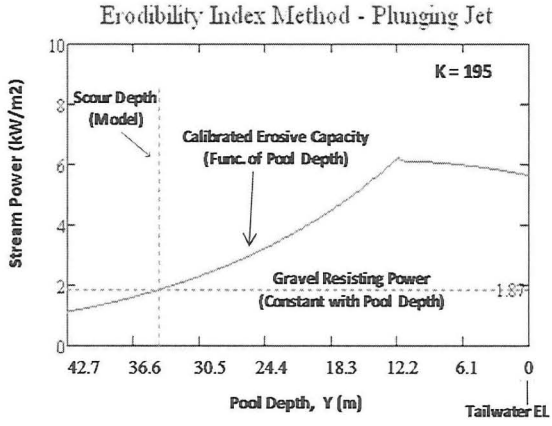

Figure 4. Example of erosive capacity calibration for revised PMF discharge.

Material Resistance

For the calibration, the erosion resistance provided by the gravel in the physical model study could be determined from the critical shear resistance calculated using the Shields parameter (1936) for cohesionless materials.

$$\tau_c = \theta_c \cdot (\rho_s - \rho) \cdot g \cdot d$$

Where:

θ_c = critical Shields parameter for rough turbulent flow = 0.06 (dimensionless).

ρ_s = particle density (kg/m^3).

ρ = water density (kg/m^3).

g = acceleration due to gravity (m/s^2).

d = diameter of gravel used in physical model = 0.01 m.

Using the scale law for stream power between model and prototype, the prototype resisting power of the gravel could be calculated using the following equation from Annandale (2006):

$$P_{cp} = 7.853 \cdot \rho \cdot \left(\sqrt{\frac{\tau_c}{\rho}}\right)^3 \cdot L_s^{\frac{3}{2}}$$

Where:

L_s = model scale = 36 (dimensionless). This value is raised to an exponent of three-halves to covert from model resisting power to prototype resisting power.

Once the calculated erosive capacity has been calibrated with the model scour results (based on the prototype resisting power of the gravel), the actual rock resistance can be inserted into the plunge pool scour module to determine a revised estimate for scour depth. Rock erodibility can be determined using the EIM (Annandale, 1995): The erodibility index, K_h, can be defined as:

$$K_h = M_s \cdot K_b \cdot K_d \cdot J_s$$

Where:

M_s = mass strength number.

K_b = block/particle size number. For rock, K_b = RQD/J_n, where RQD is the rock quality designation and J_n is the joint set number.

K_d = discontinuity/interparticle bond shear strength number. For rock, $K_d = J_r/J_a$, where J_r is the joint roughness number and J_a is the joint alteration number.

J_s = relative ground structure number.

The critical resisting stream power, P_c (W/m^2), of rock materials may be quantified using the following equation from Annandale (2006):

$$P_c = 1000 \cdot K_h^{0.75}$$

As stated above, three main rock types are found within the stilling basin: orthoquartzite, interbedded shale and orthoquartzite, and claystone. The more massive orthoquartzite layers are classified as hard to very hard rock and were determined to have a relatively high resistance to erosion. Conversely, shale layers are classified as soft to very soft rock and were found to have a relatively low erosion resistance. As indicated in Figure 5, the size of individual shale blocks is considerably smaller than those of the massive orthoquartzite units, contributing further to the difference in capacity to resist erosion. Although orthoquartzite layers are found interbedded with shale, these layers are likely to be undermined by erosion of the surrounding shale material. Subsequently, erosion resistance for the interbedded material as a whole was solely based on geologic properties for the shale.

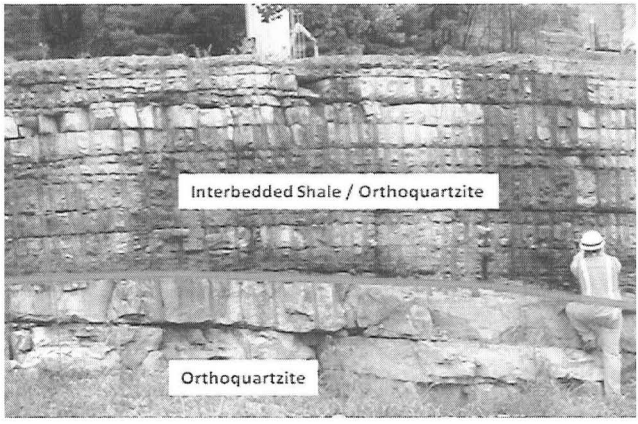

Figure 5. Outcrop at Bluestone Dam showing contact between massive orthoquartzite (bottom) and interbedded shale / orthoquartzite (top). Photo courtesy of USACE – Huntington District, Engineering Geology Section).

Claystone material resistance is less than that of the massive orthoquartzite but greater than the interbedded material. Claystone is only encountered approximately 20 m to 33 m below the stilling basin floor. Table 1 shows the calculated high and low resisting powers provided by the different rock types as well as for the gravel in the physical model study.

Table 1. Material resisting power

Rock Formation	Erodibility Index		Resisting Power (kW/m2)	
	High	*Low*	*High*	*Low*
Orthoquartzite	1199	178	204	49
Interbedded Orthoquartzite / Shale	2.24	0.47	1.83	0.57
Claystone	204	43	54	17
1:36 Scale Model Gravel (Prototype)	2.30		1.87	

Rock Scour Prediction Results

Comparison of calibrated erosive capacity for the shooting jet with the actual rock resistance yielded revised estimates of scour depth in the stilling basin. Figure 6 shows interpreted scour profiles for different discharges above the original design discharge up to the revised PMF (indicated by conditions (CN) 7 – 11) for a typical cross-section through one of the dam monoliths.

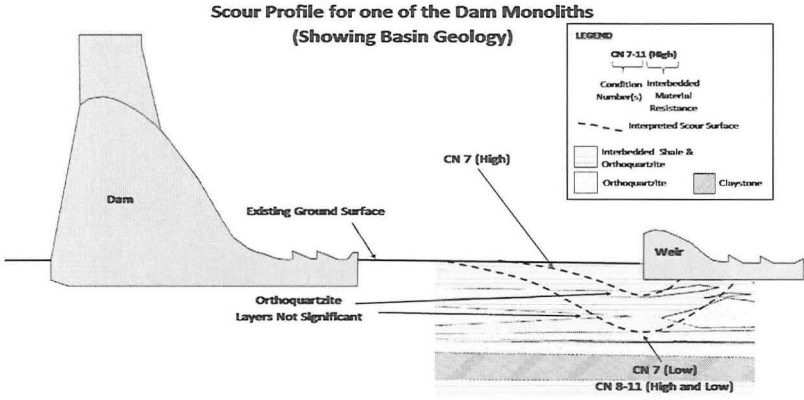

Figure 6. Scour results for typical section (Note profiles are interpreted; only the maximum depth is calculated). Geology and typical section from USACE (2003a).

For all flows analyzed, only interbedded shale material could be eroded. As indicated in Figure 6, layers of intact orthoquartzite exist, however, if these layers were not of sufficient thickness (i.e., approximately 1 m to 2 m), they were considered capable of being eroded by being undermined.

Note that the high resisting power of the interbedded shale (1.83 kW/m^2) is nearly identical to the prototype resisting power provided by the gravel (1.87 kW/m^2), which this suggests that the scour depths witnessed in the physical model could be relatively accurate for actual conditions. Should interbedded shale resistance be

closer to the low value (0.57 kW/m^2), scour depths could be deeper than those predicted by the physical model.

Figure 7 shows the different values obtained for the calibration factor, *K*, applied to the calculated erosive capacity for varying discharges above the original design. As indicated, the calibration factor begins to decrease rapidly for increasing discharge. This suggests two potential conclusions 1) more energy is dissipated for lower flows, and 2) higher flows are better represented by the plunging jet module. Values of *K* for all flows above the original design discharge are relatively high (i.e., between 95 and 245) indicating a significant amount of erosive capacity is lost. As mentioned above, this could potentially be attributed to a reduction in discharge from an unknown amount of flow in the jet going over the stilling basin weir or energy being dissipated from flow impacting apron baffles and the upstream side of the stilling basin weir.

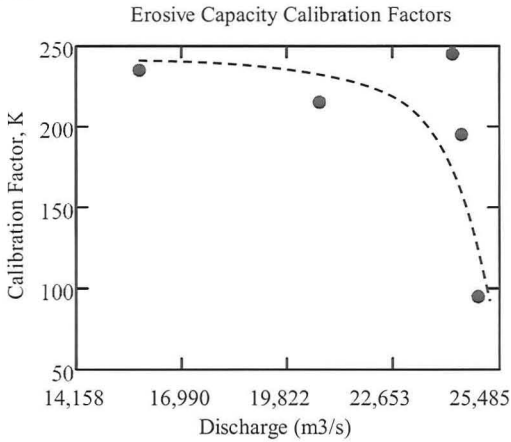

Figure 7. Erosive capacity calibration factors based on 1:36 scale hydraulic model.

Conclusions and Discussion

Flow conditions for discharges above the original design discharge in the Bluestone Dam stilling basin are unique, but loosely akin to a shooting jet into a plunge pool. As such, jet and plunge pool theories were applied in conjunction with physical hydraulic model study results to determine representative rock scour estimates for flows within the stilling.

Based on the results of the analysis, scour depths within the stilling basin can likely be equal to or greater than those witnessed in the physical model. The theoretical depths calculated are deemed to be the most representative of actual scour conditions likely to exist as the actual rock resistance was incorporated using Annandale's EIM.

The analysis was not without limitation. Most significantly, it was assumed that the scour-hole geometry (and subsequently the erosive capacity within the pool)

for the gravel material in the physical hydraulic model would be similar to that formed in the rock in the actual stilling basin. In actuality, because the materials are different, it would be reasonable to assume scour-hole shapes would different with dissimilar flow patterns and ultimately varying erosive capacities.

In spite of this, it is felt that the above methodology provides a reasonable and representative solution to a scour problem with unique and complex hydraulic flow conditions.

Acknowledgements

The authors would like to thank Mr. Michael McCray and Mr. Stephen Spoor (USACE – Huntington District) as well as Mr. Jeffery Dingrando (Stantec) for their collaboration on the project and their cooperation with this paper.

References

Annandale, G.W. (2006). *Scour Technology*. New York, McGraw-Hill.

Annandale, G.W. (1995). "Erodibility." *J. Hyd. Res.* 33, 471-494.

Bollaert, E. (2002). Transient Water Pressures in Joints and Formation of Rock Scour due to High-Velocity Jet Impact, *PhD Thesis: Communication 13*, Laboratory of Hydraulic Constructions, Swiss Federal Institute of Technology, Lausanne, Switzerland.

Castillo, L.G., Puertas, J. and J. Dolz. (2007). Contribution to discussion of Bollaert and Schleiss' paper "Scour of rock due to the impact of plunging jet Part 1: A state-of-the-art review". *J. Hyd. Res.* 45, 853-858.

Ervine, D.A., H.T. Falvey, and W. Withers. (1997). "Pressure Fluctuations on Plunge Pool Floors". *J. Hyd. Res.* 35, 257-279.

George, M. F. and G. W. Annandale. (2006a). "Kariba Dam Plunge Pool Scour." *Proc., 3rd Int. Conf. on Scour and Erosion*, Amsterdam, Netherlands.

George, M. F. and G. W. Annandale. (2006b). "Dam Failure by Rock Scour: Evaluation & Prevention (A Case Study)." *Proc., 41st U.S. Rock Mechanics Symposium (GoldenRocks 2006)*, Golden, CO, USA.

George, M. F. and G. W. Annandale. (2008). "Decreasing Scour Potential Downstream of Overtopping Dams Using Crest Modifications." *Proc., 4th Int. Conf. on Scour and Erosion*. Tokyo, Japan.

Lund, G., M. F. George, H. T. Falvey, G. W. Annandale and D. Lopez. (2008). "Eagle Nest Dam: Hydraulic Model Study of Flood Overtopping." *Proc., Conf. on Dam Safety*, ASDSO, Palm Springs, CA, USA.

Shields, A. (1936). "Anwendung der Aehnlichkeitsmechanik und der Turbulenz Forschung auf die Geschiebebewegung". Mitt. der Preussische Versuchanstalt für Wasserbau und Schiffbau, Berlin, Germany, No. 26.

United States Army Corps of Engineers (USACE) Huntington District. (2003a). "Appendix A" *Bluestone Dam Design Document Report (DDR)*.

United States Army Corps of Engineers (USACE) Huntington District. (2003b). "Appendix B: Hydrology & Hydraulics, Annex B – Bluestone Lake Dam, Baffle Blocks and Tailrace Study." *Bluestone Dam Design Document Report (DDR)*.

Numerical Modeling of Scour at Bridge Foundations on Rock

E.F.R. Bollaert[1], M. ASCE

[1] President, AquaVision Engineering, Chemin des Champs-Courbes 1, CH-1024 Ecublens, Switzerland, PH +41(0)797751761, email: erik.bollaert@aquavision-eng.ch

ABSTRACT

The present paper presents an application of the Comprehensive Scour Model (CSM) to quarrying and plucking of fractured rock at bridge piers. Numerical modeling of rock block plucking has been performed within the framework of the National Cooperative Highway Research Program Project NCHRP –24-29.

A two-phase transient numerical model simulates the potential movements of the block as a function of flow turbulence and stream power in the scour hole around the bridge pier. The hydraulic action on the rock blocks is automatically adapted during formation and growth of the scour hole.

Both the ultimate scour depth and the scour threshold flow velocity are determined as a function of the shape, dimensions and protrusion of the rock block, of the average upstream river bed slope and of the angle of the rock joints.

The numerical model points out the influence of turbulent eddies and block protrusion on rock block uplift.

INTRODUCTION

This paper describes a combined analytical-numerical method developed to assess the hydrodynamic uplift of rock blocks generated by turbulent flows at bridge piers founded on rock.

The method describes and computes the physics that are responsible for block ejection and provides an estimate of the ultimate depth of scour during floods at a bridge pier founded in fractured rock.

The method is based on a numerical model that has initially been developed for rock scour in plunge pools and stilling basins downstream of high-head dams (Bollaert, 2004). The equations defining turbulent pressure fluctuations at the water-rock interface have been adapted to reflect the particular flow situation in a scour hole near a bridge pier.

In the following, the hydrodynamic and geomechanic model parameters are first described in a simplified manner. Next, the numerical modeling procedure is outlined as well as the main results in terms of ultimate scour depth and critical scour velocity.

HYDRODYNAMIC PARAMETERS

Upstream of the bridge pier

The method uses a physical model based relationship for the erosive action of the flow inside the scour hole by using the stream power SP_a ([W/m^2]) (Figure 1) of the

approach flow. This parameter is derived from the base hydraulic parameters as follows:

$$SP_a = V_a \cdot \tau_a$$

in which V_a [m/s] stands for the approach flow velocity and τ_a [N/m^2] stands for the average wall shear stress upstream. SP_h, V_h and τ_h are the corresponding stream power, velocity and shear stress in the scour hole at the pier base. In Figure 1, n stands for the number of rock block layers, horizontal and vertical lines represent the joint planes between the blocks and the black circles represent joint plane intersections or block corners. The terms $p_{i,k}(t)$ and $p_{i+1,k}(t)$ stand for pressure fluctuations entering the joint planes via the water-rock interface.

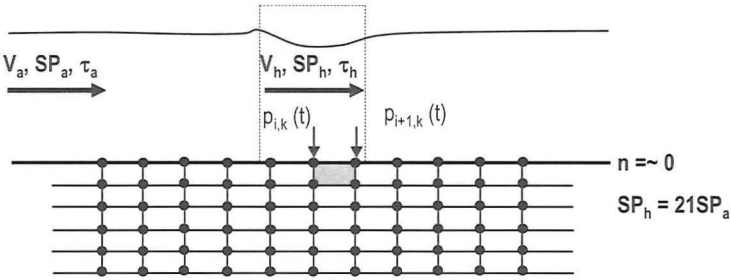

Figure 1. Hydrodynamic parameters at bridge pier founded on rock (at start of scour formation).

Beside the available stream power upstream, parameters used are written:

$SP_{a,adj} = k_1 \cdot k_2 \cdot SP_a$	=	adjusted approach stream power
k_1	=	parameter for pier shape (HEC-18)
k_2	=	parameter for flow attack angle (HEC-18)

The approach stream power SP_a is adjusted by means of the non-dimensional parameters k_1 and k_2, which account for the pier shape and the flow attack angle respectively following HEC-18 (Richardson et al., 1993). Average flow velocity and bottom shear stress are computed based on the unitary discharge q [m^3/s/m], the bottom slope S [m/m] and the Manning roughness coefficient n [s/m$^{1/3}$]. The range of flow conditions tested is summarized at Table 1 for three types of flows:

1. Steep Slope Flood Flow (SSFF)
2. Flood Flow (FF)
3. Normal High Flow (NHF)

Steep bottom slopes are between 1 and 10%, while normal bottom slopes are between 0.05 and 1 %. Unitary discharges range from 2 to 50 [$m^3/s/m$]. Manning roughness n_M is between 0.03 and 0.065 [$s/m^{1/3}$], depending on the tested slopes.

Table 1. Parameter values for the flow conditions approaching the bridge pier.

Conditions	N°	q [m^2/s]	S [m/m]	n_M [$s/m^{1/3}$]	SP_a [W/m^2]
NHF	1	5.0	0.00005	0.030	2
	2	5.0	0.00010	0.030	5
	3	10.0	0.00010	0.030	10
	4	5.0	0.00050	0.030	25
FF	1	10	0.00005	0.030	5
	2	20	0.00005	0.030	10
	3	50	0.00005	0.030	25
	4	10	0.00050	0.030	49
	5	20	0.00050	0.030	98
	6	50	0.00050	0.030	245
	7	10	0.00100	0.030	98
	8	20	0.00100	0.030	196
	9	50	0.00100	0.030	491
SSFF	1	2	0.01	0.065	196
	2	10	0.01	0.065	981
	3	15	0.01	0.065	1472
	4	2	0.05	0.065	981
	5	10	0.05	0.065	4905
	6	15	0.05	0.065	7358
	7	2	0.10	0.065	1962
	8	10	0.10	0.065	9810
	9	15	0.10	0.065	14715

At the bridge pier

As shown in Figure 1, the approach stream power SP_a is transformed into its corresponding stream power SP_h acting locally at the bottom of the scour hole, near the bridge pier. The relation between the local stream power and the scour hole depth and shape has been determined by physical modeling in the 1990's (FHWA research; Smith, 1994; Smith & Annandale, 1995) and has been adapted here to match with rocky foundations:

$$SP_h/SP_a = 2.6217(n*h_b/D)^{(-0.6945)}$$

in which h_b [m] is the rock block height, D [m] is the bridge pier diameter and n [-] stands for the number of horizontal layers that have been scoured. For example, at start of scour formation, the available and turbulent stream power at the bottom next to the bridge pier are considered to be about 21 times the corresponding stream power in the river upstream.

During scour hole formation, this stream power ratio reduces following the equation relating SP_h to SP_a. For example, for n = 4, h_b = 0.5 m and D = 2 m, Figure 2 shows that SP_h is reduced to only 2.62 times SP_a. Hence, this progressive reduction in stream power in the scour hole allows defining the corresponding local flow velocity V_h [m/s], the local kinetic energy E_h [m], and the local wall shear stress τ_h [N/m^2].

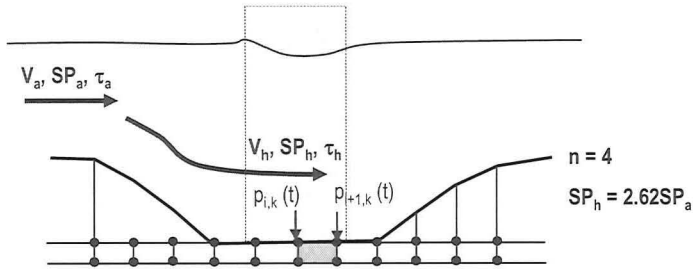

Figure 2. Hydrodynamic parameters at bridge pier founded on rock (during scour hole formation).

The local kinetic energy in the scour hole E_h is used to define the quasi-steady pressure field around a rock block near the bridge pier. These pressures are expressed in [m] by multiplying E_h with non-dimensional pressure coefficients CP. The pressure coefficients depend on the protrusion of the rock block compared to its surroundings as well as on the orientation of the joints between the blocks compared to the flow direction.

Following Figure 3 and based on Reinius (1986) and USBR (2007), the following simplified range of CP values has been used during the computations:

$CP_6 = CP_7 = \sim 0$
$CP_5 = CP_8 = 0.0$, 0.5 or 1.0, directly depending on offset of block
$CP_{up,net}$ = Average (CP6;CP7) – Average (CP5;CP8)

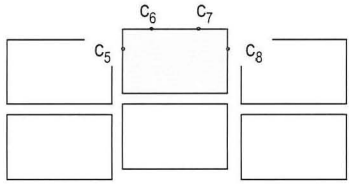

Figure 3. Location of dynamic pressure coefficients used to quantify quasi-steady pressures around a rock block (based on Reinius, 1986).

Next, the bottom shear stress τ_h is used to determine the RMS (root-mean-square) and extreme pressure fluctuations on a rock block in the scour hole near the bridge pier. Based on Emmerling (1973), the following expressions are used:

$$p' = 3 \cdot \tau_h$$
$$p+ = 18 \cdot \tau_h$$

By combining both quasi-steady pressures and turbulent pressure fluctuations, the total dynamic pressure signal on the rock blocks can be defined. For simplicity, a sinusoidal pressure shape has been used, defined as follows (see Figure 4):

$$p(t) = \frac{1}{2} \cdot B \cdot \sin(\omega \cdot t) + C$$

t = time duration
$B = p^+$ = maximum positive deviation from quasi-steady pressure value
$C = 0.5 \cdot p^+ + C_5 \cdot E_h$
$\omega = 2\pi f$, with f = 10 Hz

For convenience and stability during the computations, no negative total pressures have been used. Also, the sinusoidal pressure signal has been systematically applied to both joint entrances separating the rock block from the adjacent blocks (2D approach), without any time lag between both pulses (simultaneous action). Finally, the surface pressure field acting at the surface of the block (in between both joints) has been neglected. As such, the modeled pressure situation may be considered as the most critical one that might be encountered in practice. The frequency of the pressure signal has been defined at 10 Hz, corresponding to a frequency that may easily be reached in practice by macro-turbulent flow conditions (Toso & Bowers 1988).

GEOMECHANICAL PARAMETERS

The main geomechanical parameters considered during the modeling are:

1. *Block shape and dimensions*: side length of block L_b [m], height of block h_b [m], ratio L_b/h_b. The side length has been fixed at 1m, while the height has been varied (see Figure 4).

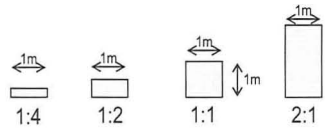

Figure 4. Modeled rock block shapes and dimensions.

2. *Joint angle with the vertical*: fixed at 0° (vertical joints) or 60° (Figure 5).

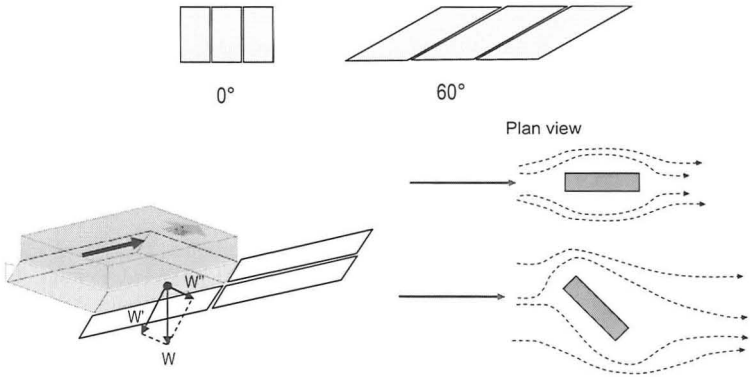

Figure 5. Modeled rock joint angles with the vertical (up) and bridge pier alignment angles with the approach flow (right).

Frictional forces inside joints have been neglected for the case of vertical joints, but have been considered for 60° joints, to account for the component of gravity that is oriented perpendicularly to the joints. Friction due to the in-situ stress field has been neglected. The following approach has been adopted:

- the weight of the block is subdivided into a component along the joint axis (W') and a component perpendicular to the joint axis (W''),
- W' stabilizes the block along its orientation of movement out of the surrounding mass,
- W'' stabilizes the block by (perpendicular) compression of the joints between the blocks and by applying a joint friction angle μ
- an additional frictional force $F = W''\mu$ is added to the computation of the net uplift force along the orientation of potential block movement
- the dip direction is not considered to influence the net uplift force, because the model does not account for the dip when defining flow deviation effects (pressures) generated by protrusion of blocks at the water-rock interface

3. *Block density*: fixed at 2650 kg/m^3.
4. *Block protrusion*: from perfectly smooth (offset = 0 cm) to very rough (offset = min. 10 cm)

BRIDGE PIER PARAMETERS

The bridge pier has been modeled in a simple manner by accounting for the following parameters:

1. *Bridge pier diameter D (or width B):* fixed at 2 m
2. *Angle of bridge pier with flow angle*: 0° or 45° (Figure 5)

The angle between the bridge pier alignment and the approach flow is accounted for by means of a k parameter that is applied to the stream power, following HEC-18 (Richardson et al., 1993). For example, for 0° and 45° angles, and a pier length to width ratio of 4, this k parameter equals 1.0 respectively 2.3.

THE BRIDGE PIER SCOUR MODEL

Model assumptions

A transient two-phase numerical modeling of quasi-steady and fluctuating turbulent pressures acting inside the joints of a single rock block has been performed (Bollaert, 2002, 2004). Figure 7 illustrates the basic configuration used for the numerical computations. The model applies a sinusoidal boundary pressure signal at the joint entrances and computes the pressure waves inside the joints. Only one single block is computed, considered to be located at the bottom of the scour hole in the vicinity of the bridge pier. Based on the block dimensions, the computations are performed layer per layer, with the layer height taken equal to the block height.

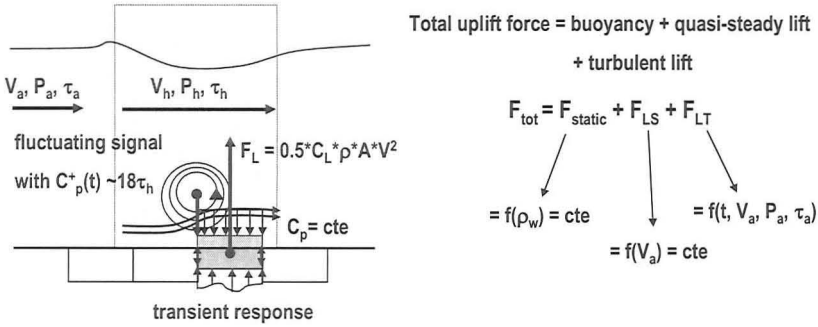

Figure 7. Uplift forces on a single rock block at a bridge pier.

Uplift or ejection of a rock block is computed by defining at each time step the total net uplift force on the block. As illustrated in Figure 7, this total uplift force is composed of three distinct components (Bollaert and Hofland, 2004):

1. static uplift = buoyancy forces
2. quasi-steady uplift = f (block protrusion, local velocity in scour hole)
3. turbulent uplift = f(local stream power, shear stresses, pressure fluctuations)

During time periods for which the net uplift force on the block is positive, the block will be submitted to a net uplift impulsion. This is then transformed into a net uplift velocity that is given to the mass of the block. Finally, the net uplift velocity is transformed into a net uplift height. The block is considered to be ejected when its net uplift height is larger than or equal to 20% of the total block height (Bollaert, 2004).

Once the single rock block is found to be ejected by the pressures, the whole layer is considered to be eroded and the next layer is computed until block uplift is less than 20 % of block height. This corresponds to the ultimate scour depth.

Output examples

First, Figure 8 compares the here computed critical uplift velocity for a range of different rock blocks with the critical uplift velocity as defined by Reinius (1986) for CP values of 0.0 and 0.5. It is thereby considered that, due to the small model scale and the way the pressures have been recorded, the Reinius (1986) approach does not consider the effect of turbulent eddies. When adding the effect of flow turbulence to the present computations, significantly lower critical velocities are observed. It has to be added that joint frictional effects have been neglected in the present analysis. In reality, critical uplift velocities may be significantly higher in presence of friction.

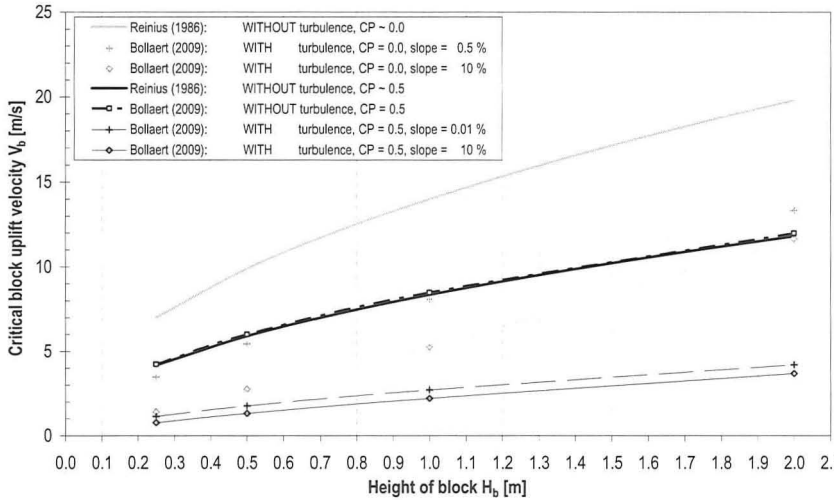

Figure 8. Comparison of critical block uplift velocities with Reinius (1986).

Second, Figure 9 illustrates the pressure signals computed over and under a 0.4 m high and 1.2 m long rock block. The block has a protrusion of 0.1 m and is impacted by a turbulent flow with a unitary discharge of 10 m^2/s and an approach flow velocity of 5.1 m/s. The lower part of Figure 9 shows that the rock block will be uplifted by a height of about 0.22 m, i.e. more than 50 % of its total height. Hence, the block may be considered ejected from the surrounding rock mass.

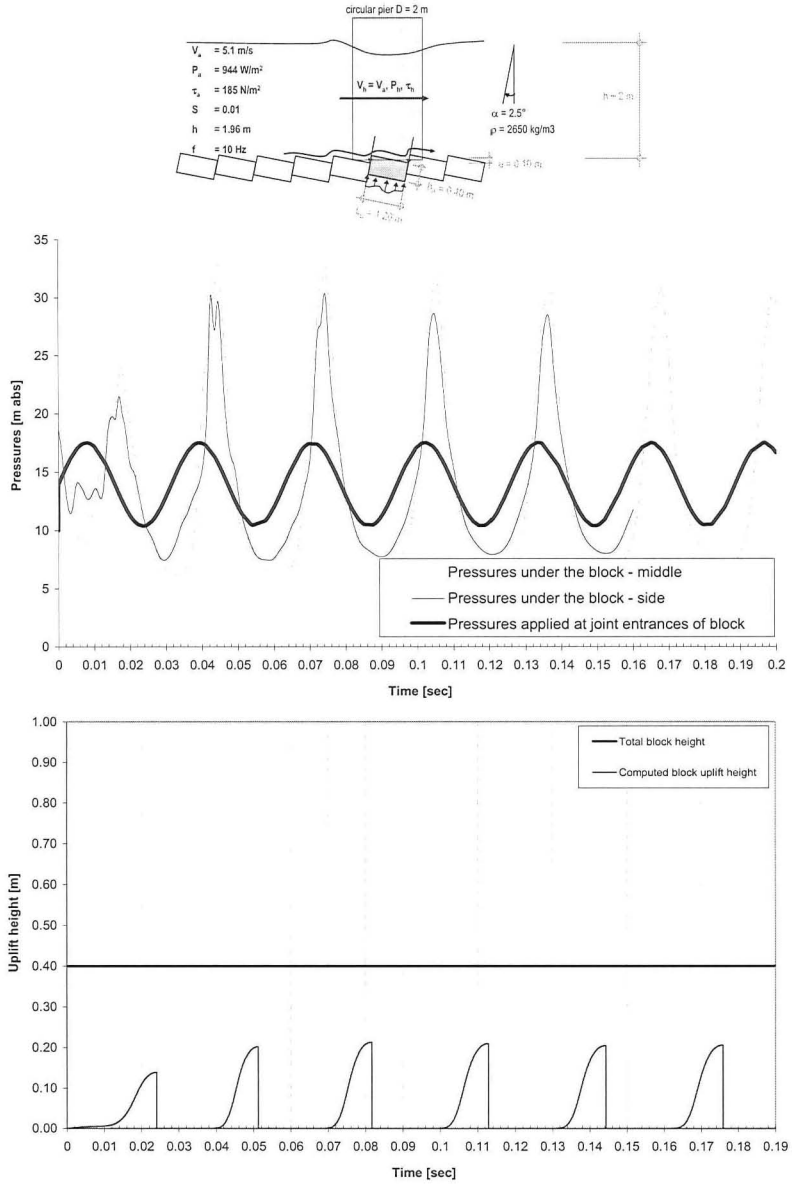

Figure 9. Pressure signals and uplift heights of a protruding rock block at a bridge pier.

CONCLUSIONS

The present application of the Comprehensive Scour Model (CSM, Bollaert 2002) to plucking of fractured rock at bridge piers has allowed simulating the potential movements of a single rock block by direct coupling of flow turbulence and stream power inside the forming scour hole with transient pressure pulses generated underneath the blocks at the bottom of the hole.

The hydraulic action on the blocks is automatically adapted during formation and growth of the scour hole. Both the ultimate scour depth and the scour threshold velocity are determined as a function of the shape, dimensions and protrusion of the rock block, of the average upstream river bed slope and of the angle of the rock joints.

Comparison with previous research on rock block uplift points out the importance of turbulent pressure fluctuations on rock block uplift. Also, block protrusion was found to significantly enhance quasi-steady uplift forces on the blocks.

For a large range of block shapes and protrusions and for different approach flow conditions (bottom slopes, stream power), the critical block uplift velocity and the ratio of the ultimate scour depth to bridge pier diameter have been determined.

ACKNOWLEDGMENT

The present numerical modeling has been performed within the framework of the National Cooperative Highway Research Program Project NCHRP 24-29.

REFERENCES

Bollaert, E.F.R. (2002). "Transient water pressures in joints and formation of rock scour due to high-velocity jet impact." *PhD Thesis N°2548*, Ecole Polytechnique Fédérale de Lausanne, Switzerland.

Bollaert, E.F.R. (2004). "A comprehensive model to evaluate scour formation in plunge pools." *Int. Journal of Hydropower & Dams*, 2004(1), pp. 94-101.

Bollaert, E.F.R. and Hofland, B. (2004). "The Influence of Flow Turbulence on Particle Movement due to Jet Impingement." *2nd Scour and Erosion Conference*, Nanyang, Singapore.

Smith, S.P. (1994). "Preliminary Procedure to Predict Bridge Scour in Bedrock." *Report N° CDOT-R-SD-94-14*, Colorado Dept of Transportation, Denver, US.

Smith, S.P. and Annandale, G.W. (1997). "Scour in Erodible Bedrock II: Erosive Power at Bridge Piers." *Proceedings of North American Water and Environmental Congress*, Anaheim, CA, US.

Schlichting, H. and Gersten, K. (2000). „Boundary Layer Theory." *8th Ed. (Revised and Enlarged)*, Springer-Verlag, New York.

Reinius (1986). "Rock Erosion." *Water Power and Dam Construction*, June 1986, pp. 43-48.

Richardson, E.V., Harrison, L.J. and Richardson, J.R. (1993). "Evaluating Scour at Bridges." *FHWA-IP-90-017*, US Department of Transportation, Washington, D.C.

USBR (2007). "Uplift and Crack Flow resulting from High Velocity Discharges over open Offset Joints." *Report DSO-07-07*, US Bureau of Reclamation, Denver.

Toso, J., Bowers, E.C. (1988). "Extreme pressures in hydraulic jump stilling basin." *Journal of Hydraulic Engineering*, ASCE, Vol. 114, N° HY8, pp. 829-843.